

# A guide to radiation damage in silicon detectors by RD50

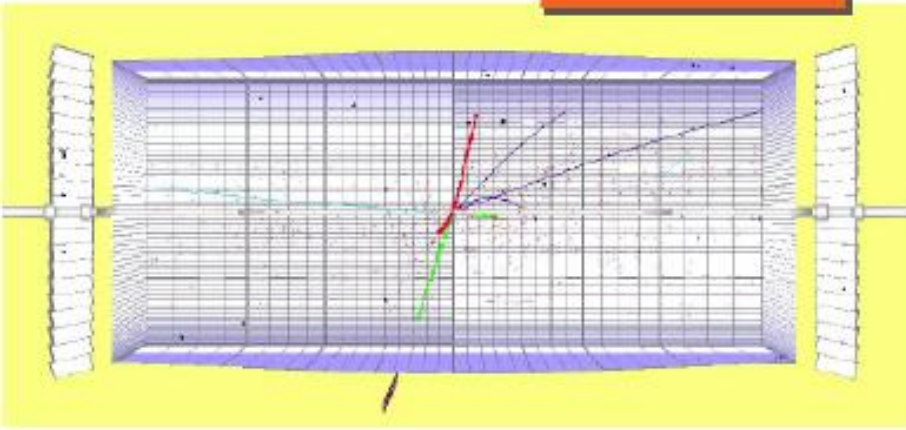
Michael Moll (CERN), Jaakko Härkönen  
(Helsinki Institute of Physics)

# Outline

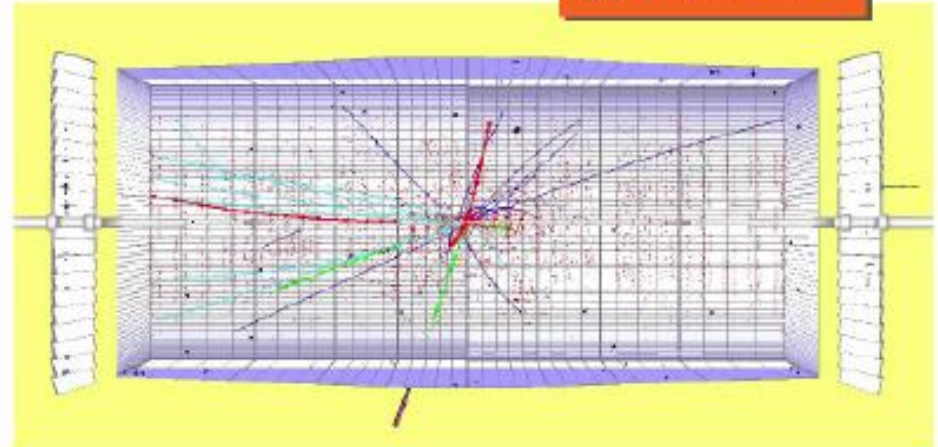
- **Motivation to develop radiation harder detectors**
  - expected radiation levels at the upgraded LHC (sLHC)
  - Radiation induced degradation of detector performance
- **Radiation Damage in Silicon Detectors**
  - Microscopic damage (crystal damage), NIEL
  - Macroscopic damage (changes in detector properties:  $N_{\text{eff}}$ ,  $I_R$ ,  $CC(V)$ )
- **Changes with time after irradiation**
  - Annealing of the detector electrical properties:  $N_{\text{eff}}$ ,  $I_R$ ,  $CCE(V)$
- **Radiation hardening of Silicon sensors**
  - Material Engineering
    - New silicon materials – FZ, MCZ, DOFZ, EPI
  - Device Engineering
    - p-in-n, n-in-n and n-in-p sensors, 3D sensors
- **Conclusions**

# The challenge: Super LHC - visually

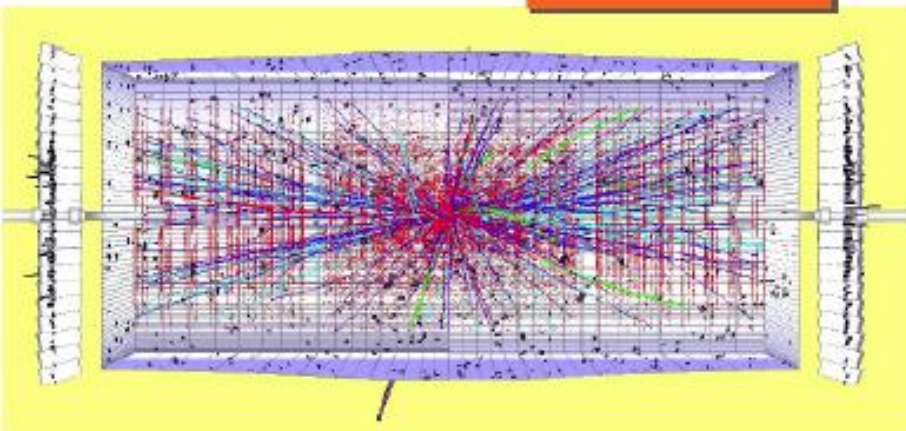
$10^{32} \text{ cm}^{-2} \text{ s}^{-1}$



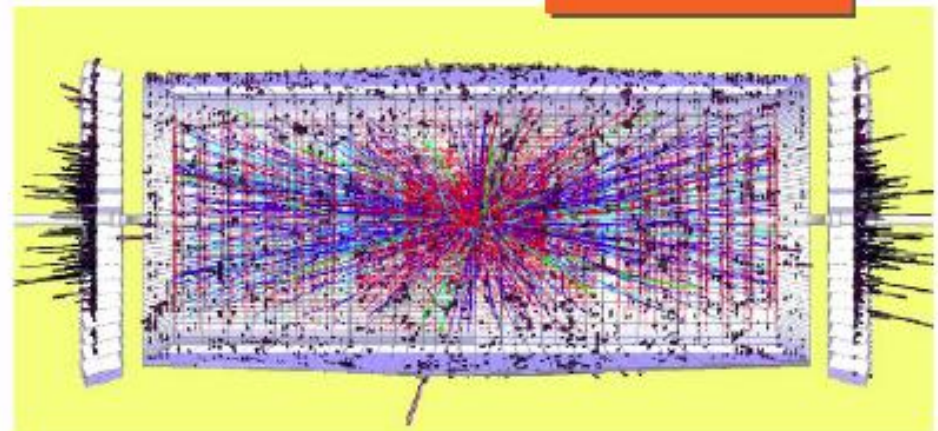
$10^{33} \text{ cm}^{-2} \text{ s}^{-1}$



$10^{34} \text{ cm}^{-2} \text{ s}^{-1}$



$10^{35} \text{ cm}^{-2} \text{ s}^{-1}$



LHC luminosity

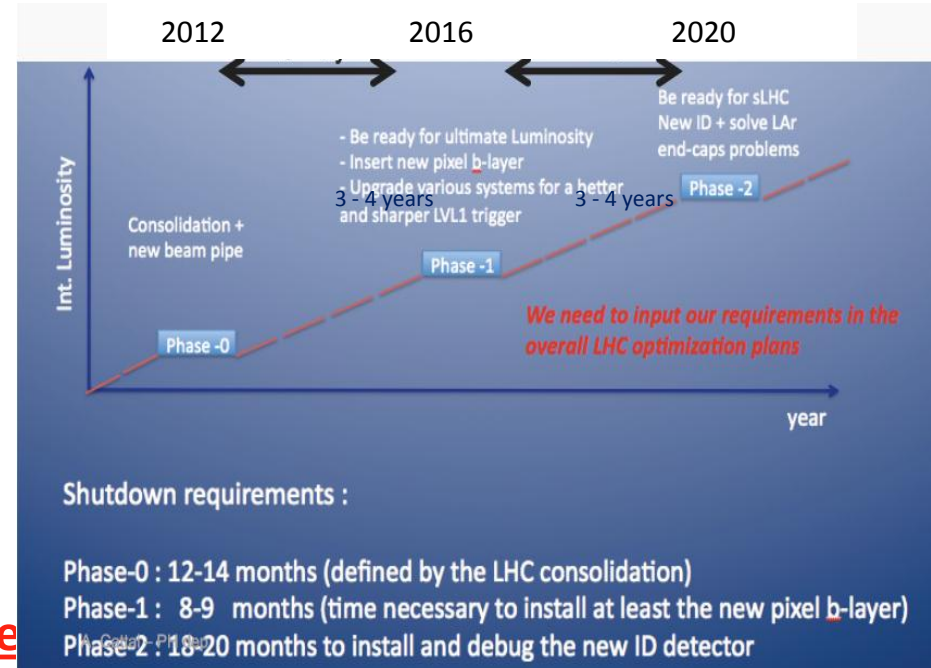
SLHC luminosity ~300-400 interactions/bx

# Upgrading the LHC for High Luminosity

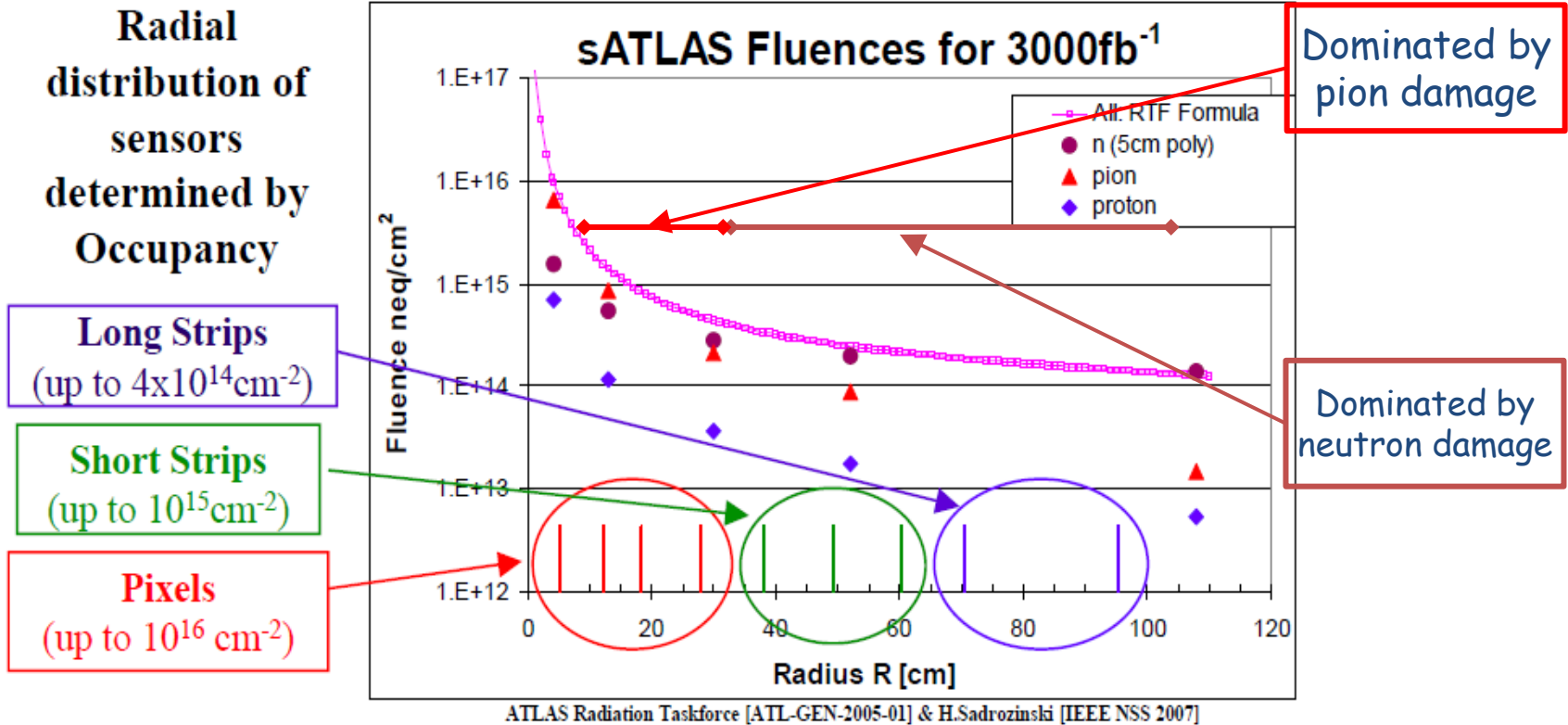
With modest investment, the **LHC can run at much higher collision rates**, greatly increasing the scope to search for new particles and study rare processes

## Expected Development in Luminosity

- Phase-I (after 5 years)
  - Up to  $\sim 60\text{fb}^{-1}/\text{year}$
  - Experiments need:
    - **New vertex detectors**
    - **New off-line electronics**
    - ...
- Phase-II (after 10 years)
  - Up to  $\sim 300\text{fb}^{-1}/\text{year}$
  - Experiments need:
    - **Complete tracker replacement**
    - **Much improved on-line filtering**
    - **New read-out for many subsystems**
    - ...



# Radiation levels expected with sLHC

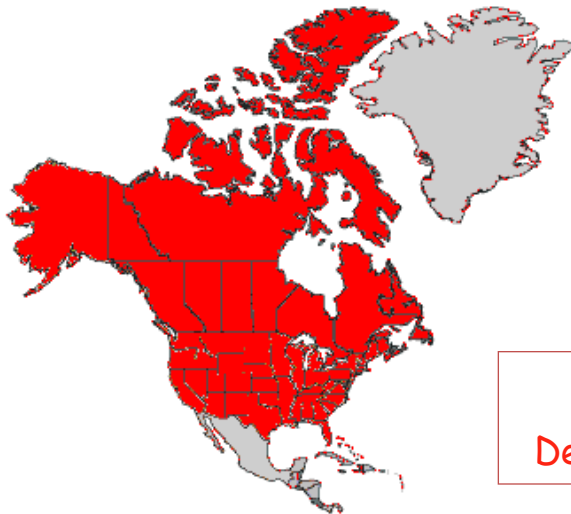
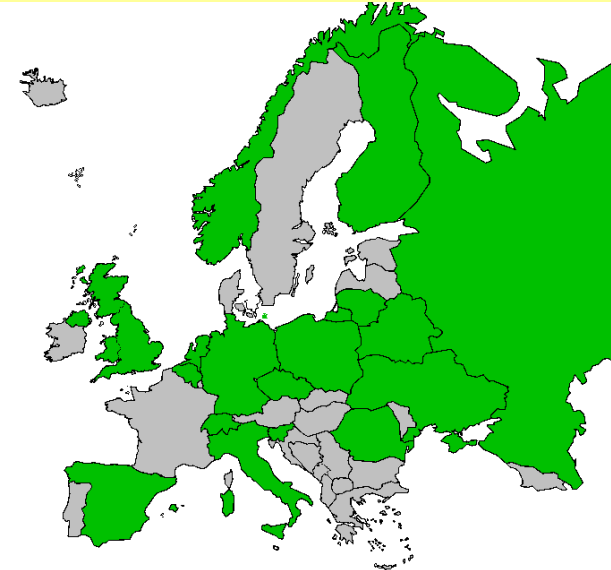


- **Radiation hardness requirements (including safety factor of 2)**
  - $2 \times 10^{16} \text{ n}_{\text{eq}}/\text{cm}^2$  for the innermost pixel layers
  - $1 \times 10^{15} \text{ n}_{\text{eq}}/\text{cm}^2$  for the innermost strip layers

# RD50 - Development of Radiation Hard Semiconductor Devices for High Luminosity Colliders

## 38 European institutes

**Belarus** (Minsk), **Belgium** (Louvain), **Czech Republic** (Prague (3x)), **Finland** (Helsinki, Lappeenranta), **Germany** (Dortmund, Erfurt, Freiburg, Hamburg, Karlsruhe, Munich), **Italy** (Bari, Florence, Padova, Perugia, Pisa, Trento), **Lithuania** (Vilnius), **Netherlands** (NIKHEF), **Norway** (Oslo (2x)), **Poland** (Warsaw(2x)), **Romania** (Bucharest (2x)), **Russia** (Moscow, St.Petersburg), **Slovenia** (Ljubljana), **Spain** (Barcelona, Valencia), **Switzerland** (CERN, PSI), **Ukraine** (Kiev), **United Kingdom** (Glasgow, Lancaster, Liverpool)



## 8 North-American institutes

**Canada** (Montreal), **USA** (BNL, Fermilab, New Mexico, Purdue, Rochester, Santa Cruz, Syracuse)

## 1 Middle East institute

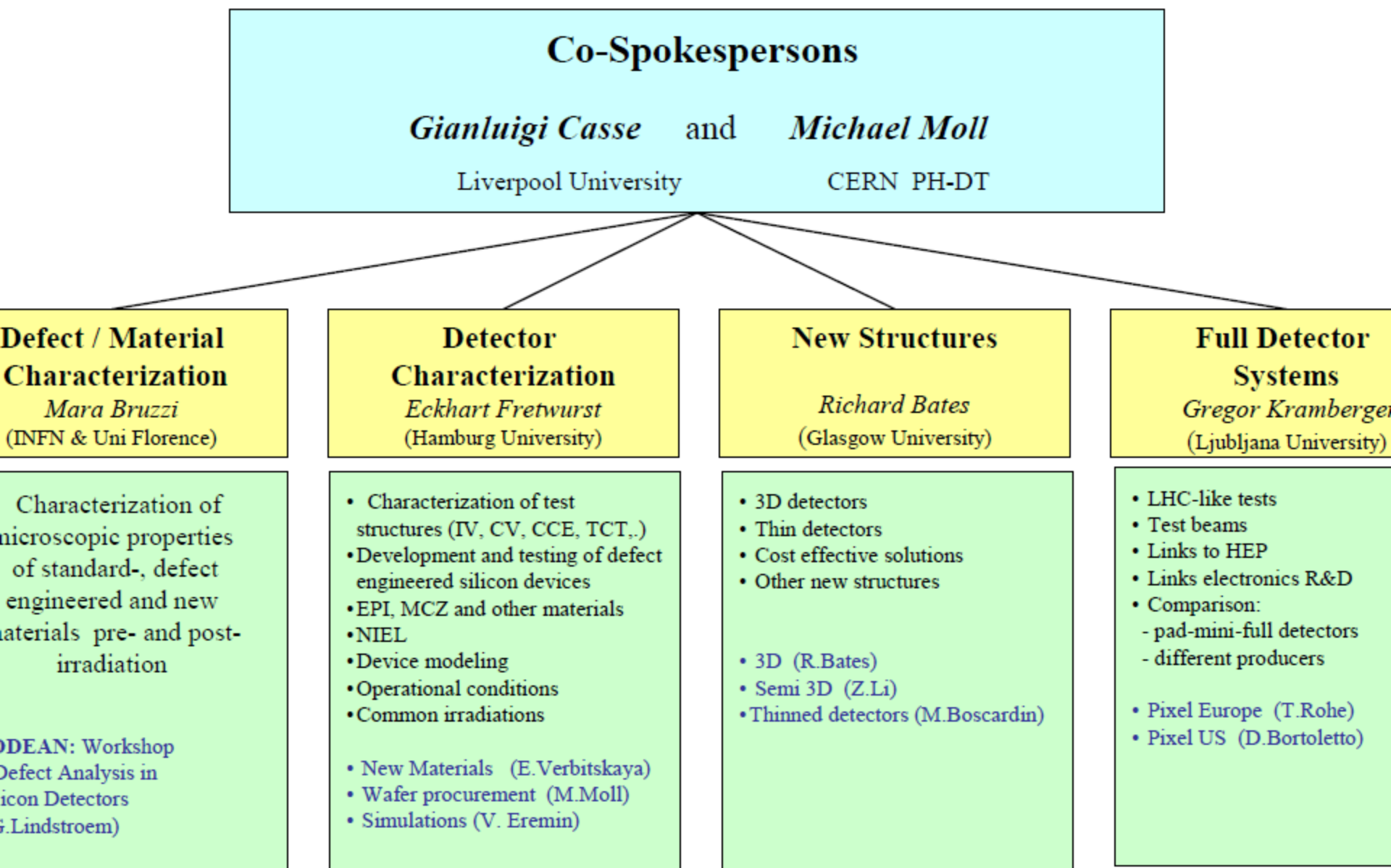
**Israel** (Tel Aviv)

257 Members from 47 Institutes

Detailed member list: <http://cern.ch/rd50>

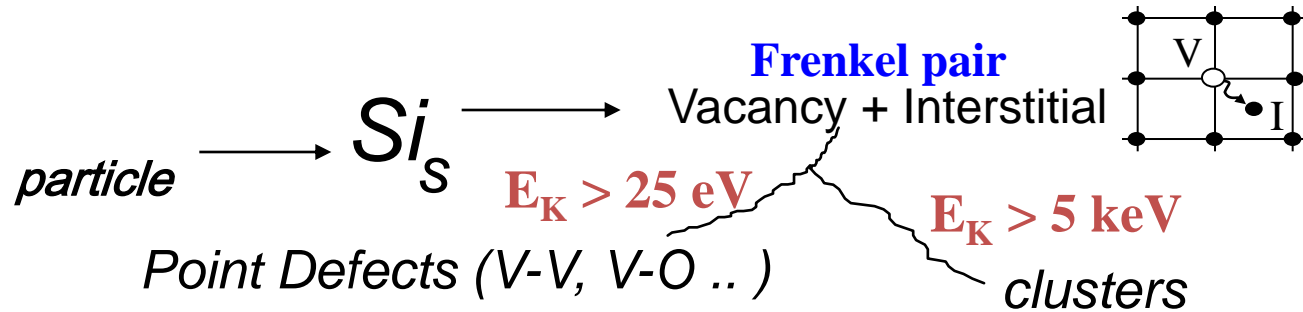
# Scientific Organization of RD50

*Development of Radiation Hard Semiconductor Devices for High Luminosity Colliders*

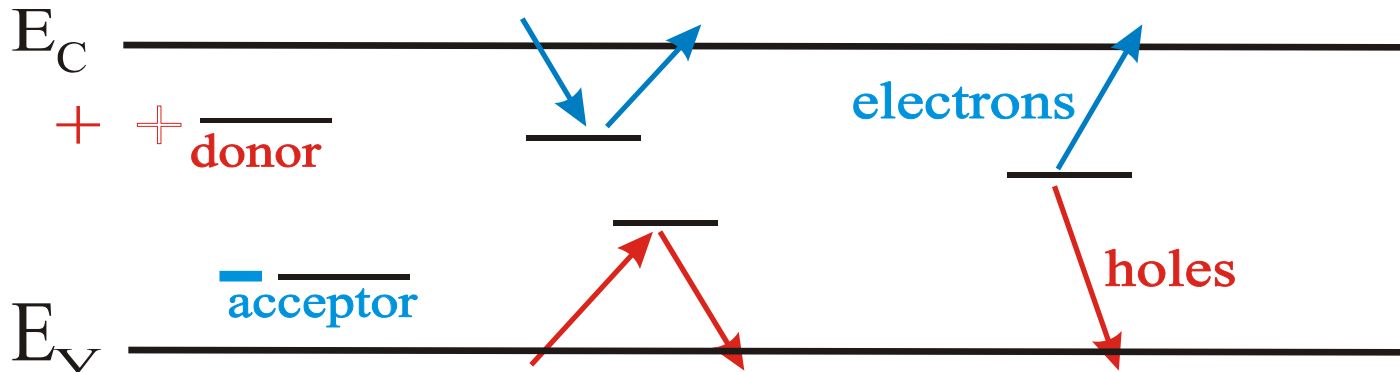


*Collaboration Board Chair & Deputy: E.Fretwurst (Hamburg) & J.Vaitkus (Vilnius), Conference committee: U.Parzefall (Freiburg)*

# Radiation induced damage



## Influence of defects on the material and device properties



**charged defects**

$\Rightarrow N_{\text{eff}}, V_{\text{dep}}$   
 e.g. donors in upper  
 and acceptors in  
 lower half of band  
 gap

**Trapping (e and h)**

$\Rightarrow \text{CCE}$   
 shallow defects do not  
 contribute at room  
 temperature due to fast  
 detrapping

**generation**

$\Rightarrow$  **leakage current**  
 Levels close to  
 midgap  
 most effective



# Vacancy amount and distribution depends on particle kind and energy

<sup>60</sup>Co-gammas

–Compton Electrons  
with max.  $E_\gamma \approx 1$  MeV  
(no cluster production)

Electrons

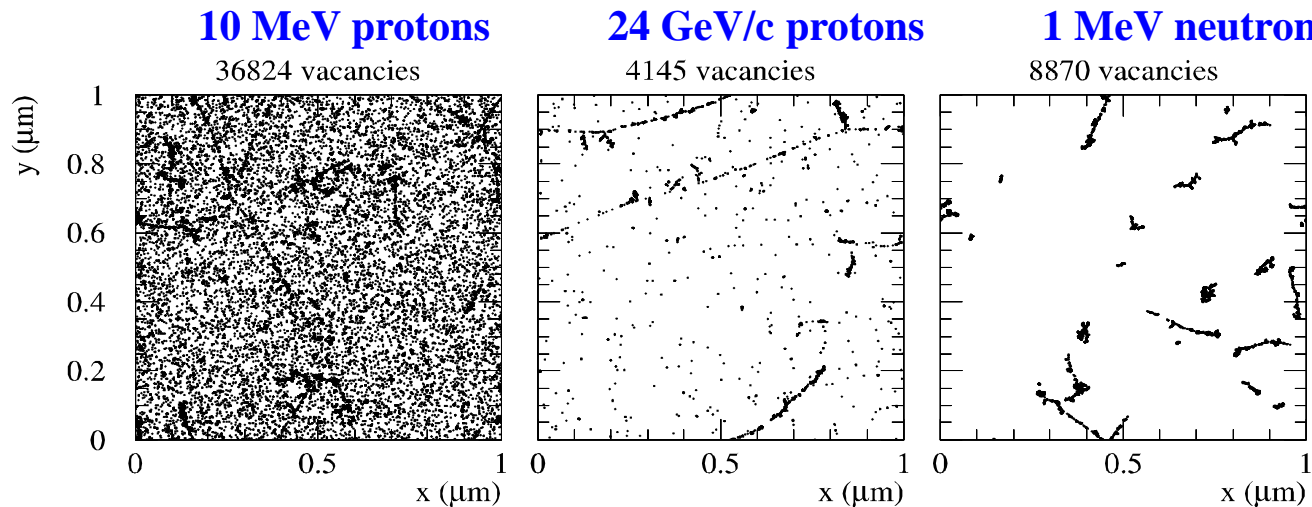
– $E_e > 255$  keV for displacement  
– $E_e > 8$  MeV for cluster

Neutrons (elastic scattering)

–  $E_n > 185$  eV for displacement  
–  $E_n > 35$  keV for cluster

Only point defects  $\longleftrightarrow$  point defects & clusters  $\longleftrightarrow$  Mainly clusters

Initial distribution of vacancies in  $(1\mu\text{m})^3$  after  $10^{14}$  particles/cm<sup>2</sup>



[Mika Huhtinen NIMA 491(2002) 194]

# How to normalize radiation damage from different particles?

- NIEL - Non Ionizing Energy Loss scaling using hardness factors

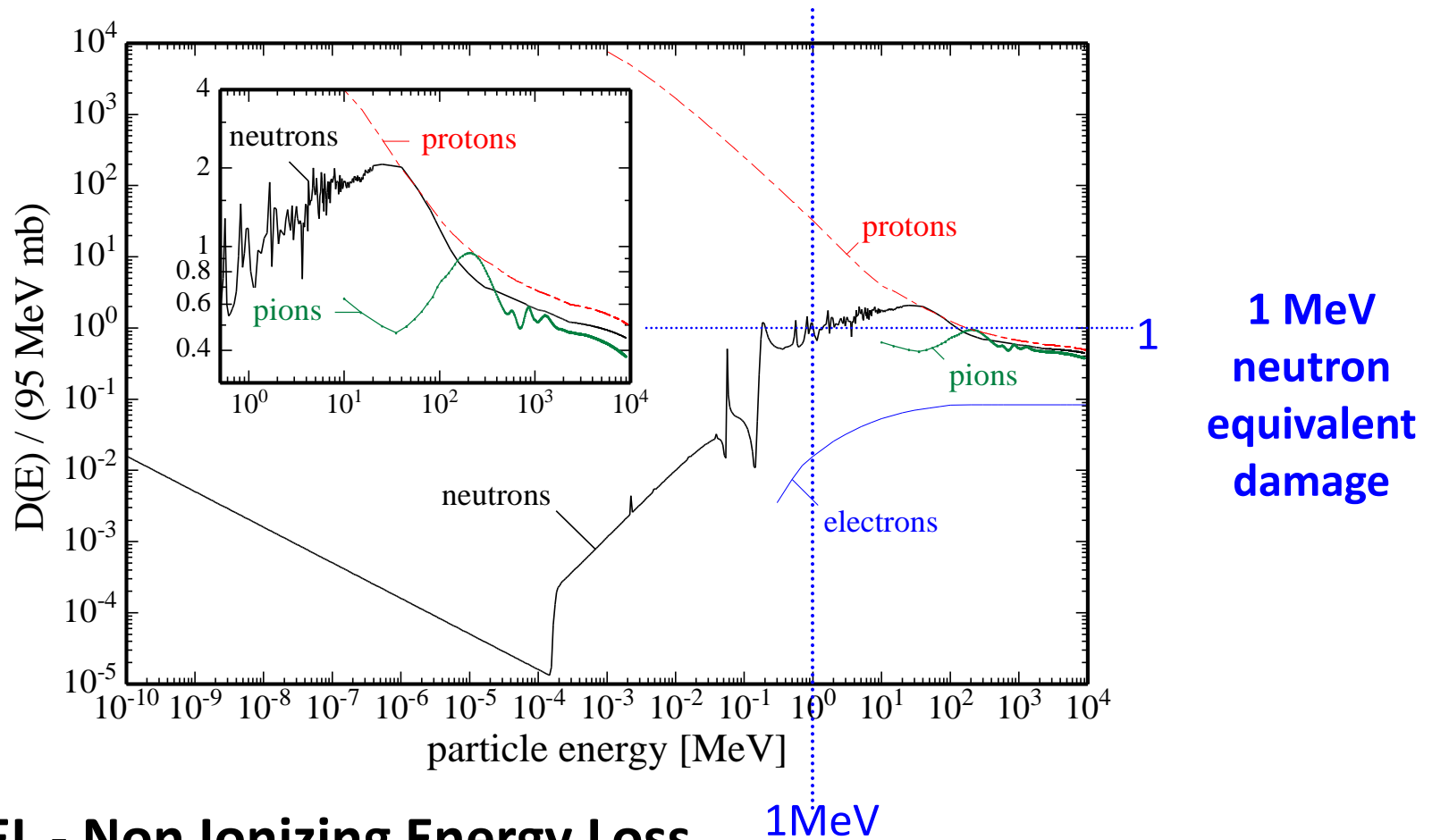
$$\kappa = \frac{1}{D(1\text{MeV neutrons})} \cdot \frac{\int D(E) \phi(E) dE}{\int \phi(E) dE}$$

**Hardness factor  $\kappa$**  of a radiation field (or monoenergetic particle) with respect to 1 MeV neutrons.

- **E** energy of particle
- **D(E)** displacement damage cross section for a certain particle at energy E  
 $D(1\text{MeV neutrons})=95 \text{ MeV}\cdot\text{mb}$
- **$\phi(E)$**  energy spectrum of radiation field

The integrals are evaluated for the interval  $[E_{\text{MIN}}, E_{\text{MAX}}]$ , being  $E_{\text{MIN}}$  and  $E_{\text{MAX}}$  the minimum and maximum cut-off energy values, respectively, and covering all particle types present in the radiation field

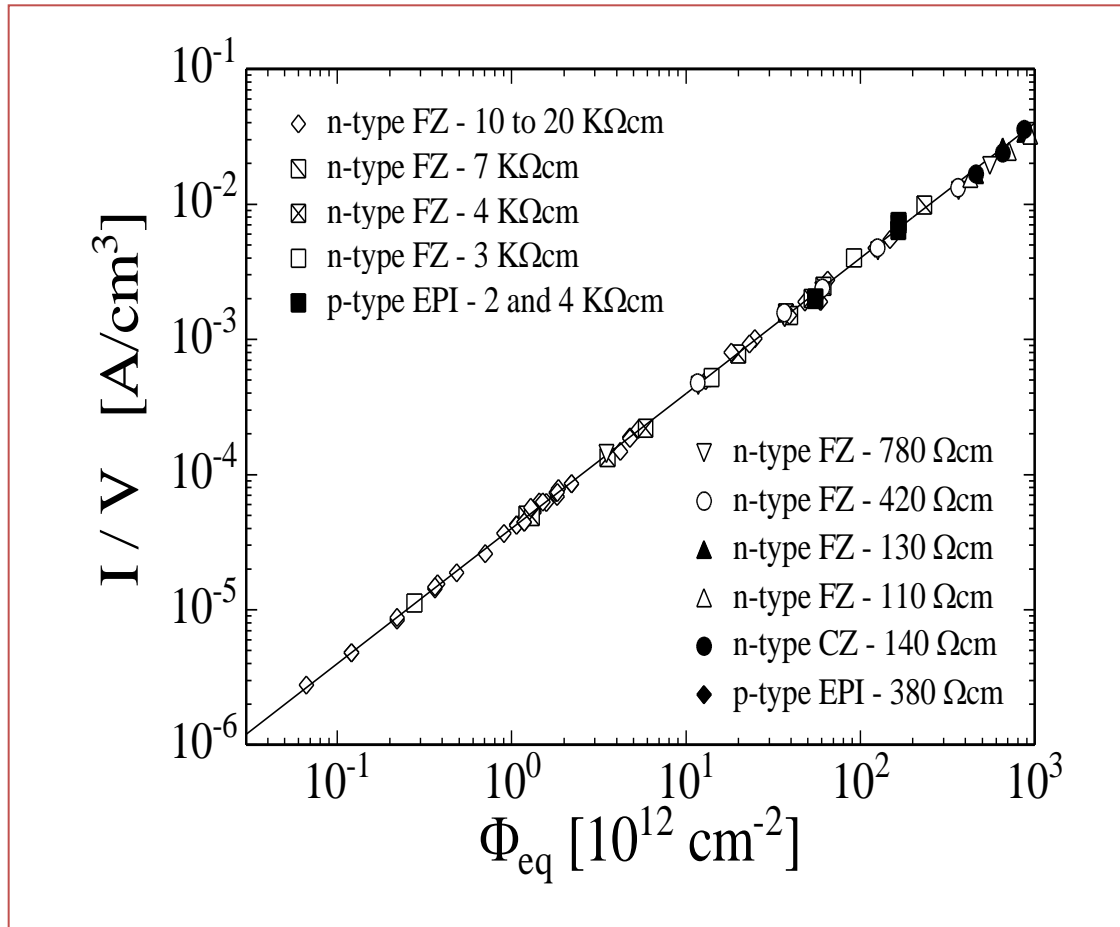
# NIEL - Displacement damage functions



- NIEL - Non Ionizing Energy Loss
- NIEL - Hypothesis: Damage parameters scale with the NIEL
  - *Be careful, does not hold for all particles & damage parameters (see later)*

# Radiation Damage: macroscopic parameters

## I. Increase of leakage current with the fluence



- Damage parameter  $\alpha$  (slope in figure):  
**Leakage current per unit volume and particle fluence**

$$\alpha = \frac{\Delta I}{V \cdot \Phi_{eq}}$$

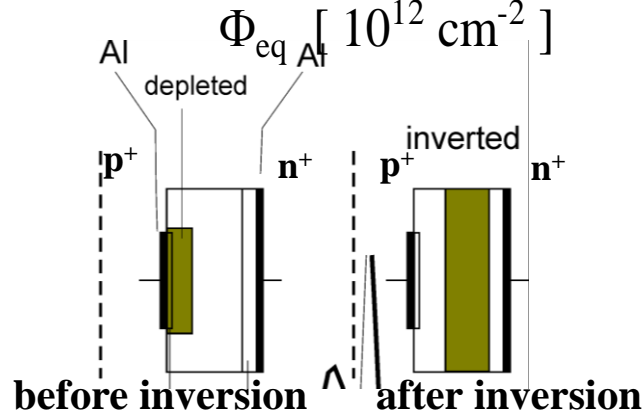
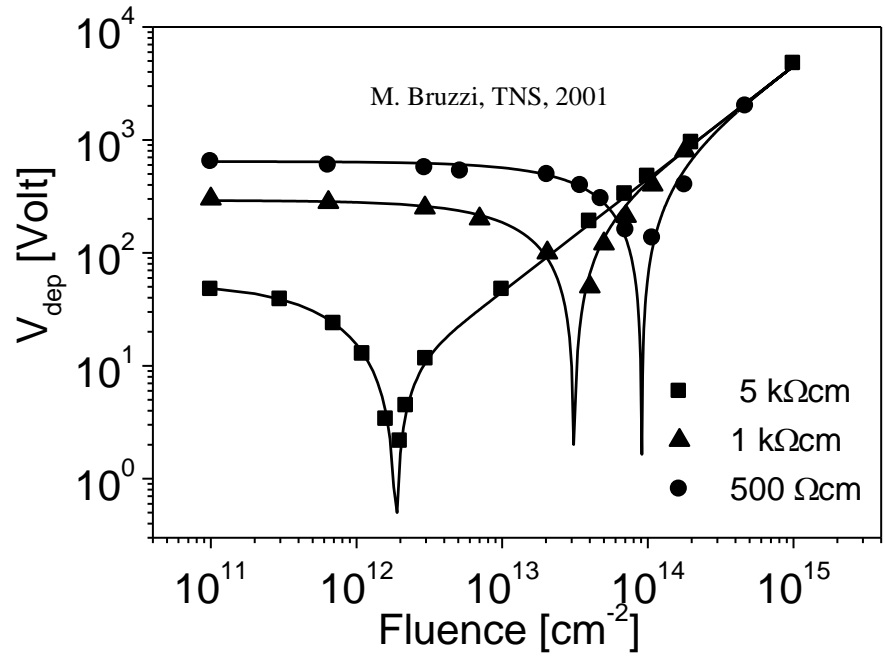
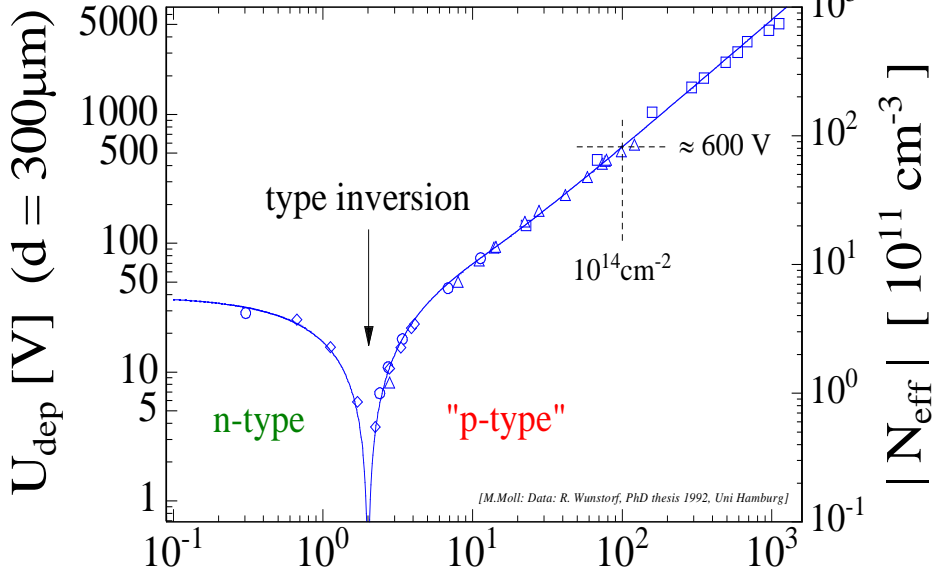
$\alpha$  independent of  $\Phi_{eq}$  and impurities  $\Rightarrow$  used for fluence calibration (NIEL-Hypothesis)

# II. Change of $V_{fd}$ and $N_{eff}$ with fluence

$$\Delta N_{eff}(\Phi) = | N_{C0}(1 - e^{-c\Phi}) - \beta \cdot \Phi |$$

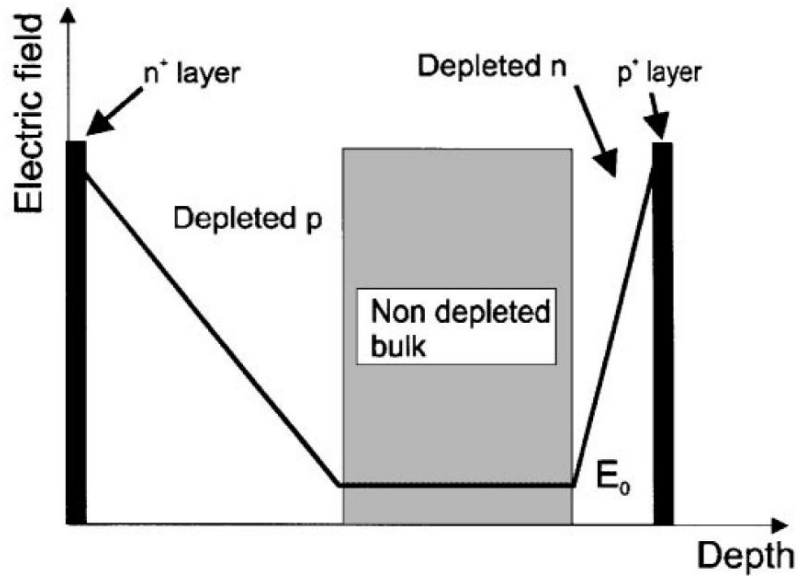
Production of acceptor like defect

Removal of the shallow dopant level



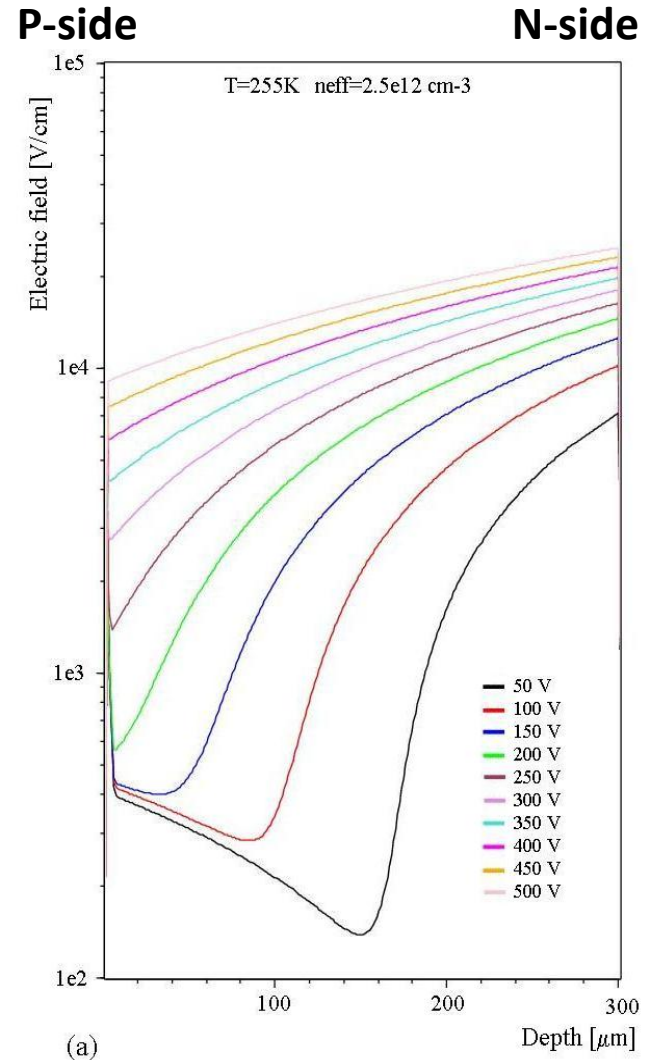
$V_{dep}$  vs. fluence plot indicates an inversion of the Space Charge Sign at high fluences

# Double Junction



In reality, after irradiation electric fields show a double junction structure with a non-depleted bulk in the middle of the sensor below the full depletion voltage

See G. Casse, et. al., NIMA 426 (1999) 140-146 and G. Kramberger, et. al., NIMA 579 (2007) 762-765 for details



ISE-TCAD simulation after  $6 \cdot 10^{14} \text{ p cm}^{-2}$

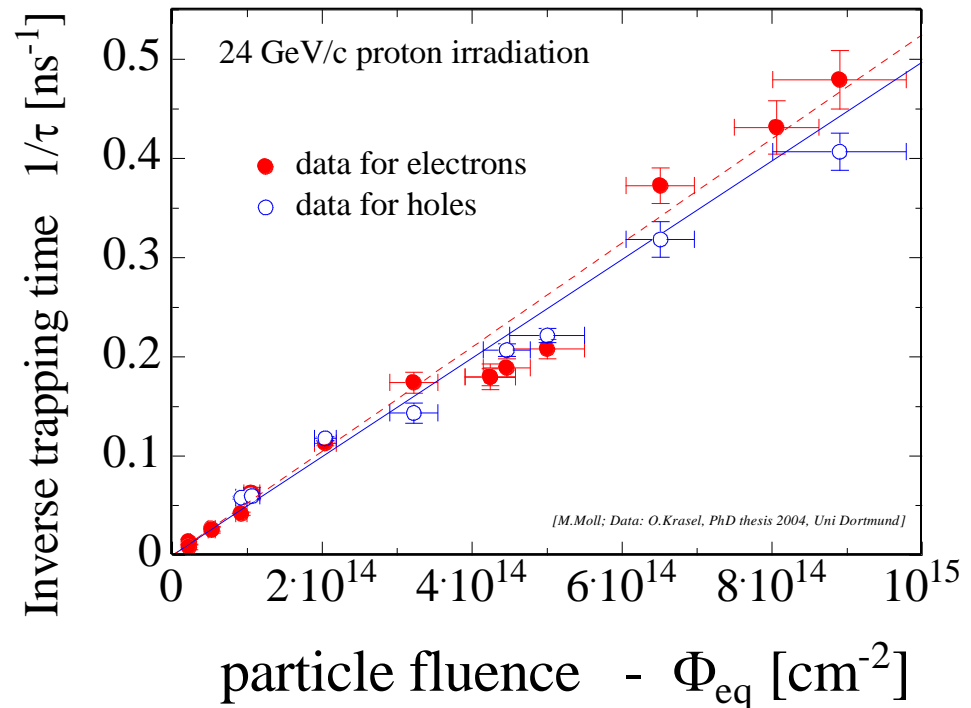
# III. Charge Collection Efficiency (CCE) degradation due to trapping

CCE degradation is mainly due to partial depletion and trapping.

Effective trapping time  $\tau_{\text{eff}}$  for electrons and holes:

$$Q_{e,h}(t) = Q_{0e,h} \exp\left(-\frac{1}{\tau_{\text{eff } e,h}} \cdot t\right) \quad \text{where} \quad \frac{1}{\tau_{\text{eff } e,h}} \propto N_{\text{defects}}$$

Increase of inverse trapping time ( $1/\tau$ ) with fluence  $\longrightarrow$



# Expected signal from charge trapping

## Effect of trapping on the Charge Collection Distance:

Expected collection distance at saturation velocity  $\lambda_{av}$  :

after  $1 \times 10^{15} \text{ n}_{eq} \text{ cm}^{-2}$ :  $240 \mu\text{m}$   
expected charge  $\sim 19 \text{ ke}$ .

$\lambda_{av}$  after  $1 \times 10^{16} \text{ n}_{eq} \text{ cm}^{-2}$ :  $25 \mu\text{m}$   
expected charge  $< 1.3 \text{ ke}$  : quite inefficient detector!

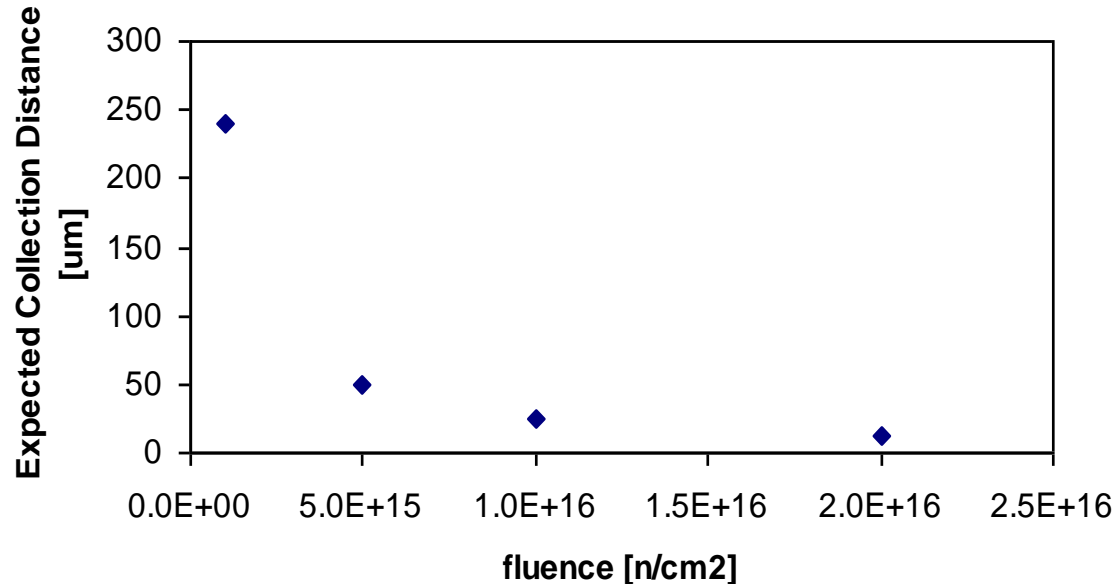
$$Q_{tc} \cong Q_0 \exp(-t_c/\tau_{tr}), \quad 1/\tau_{tr} = \beta\Phi.$$

$$v_{sat,e} \times \tau_{tr} = \lambda_{av}$$

$$\beta_e = 4.2 \text{E-}16 \text{ cm}^{-2}/\text{ns}$$

$$\beta_h = 6.1 \text{E-}16 \text{ cm}^{-2}/\text{ns}$$

G. Kramberger et al.,  
NIMA 476(2002), 645-651.





# Signal to Noise ratio Example with diodes



What is signal and what is noise?



- Landau distribution has a low energy tail
  - becomes even lower by noise broadening

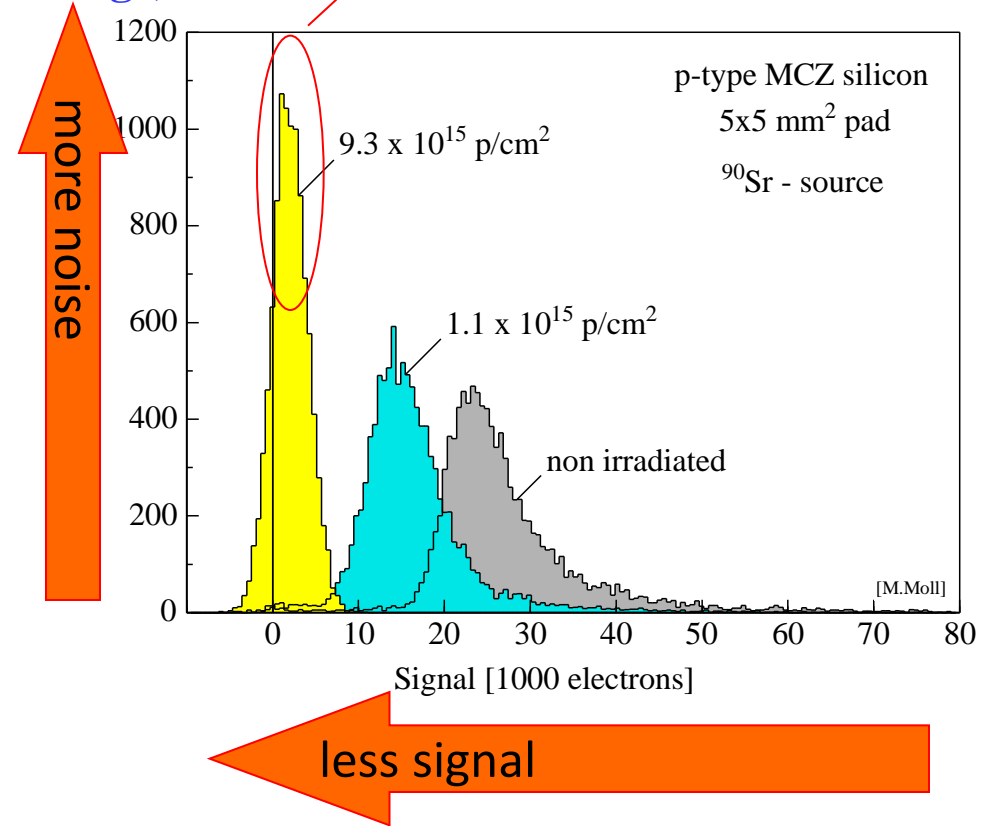
## Noise sources: (ENC = Equivalent Noise Charge)

- Capacitance  $ENC \propto C_d$

- Leakage Current  $ENC \propto \sqrt{I}$

- Thermal Noise (bias resistor)  $ENC \propto \sqrt{k_B T / R}$

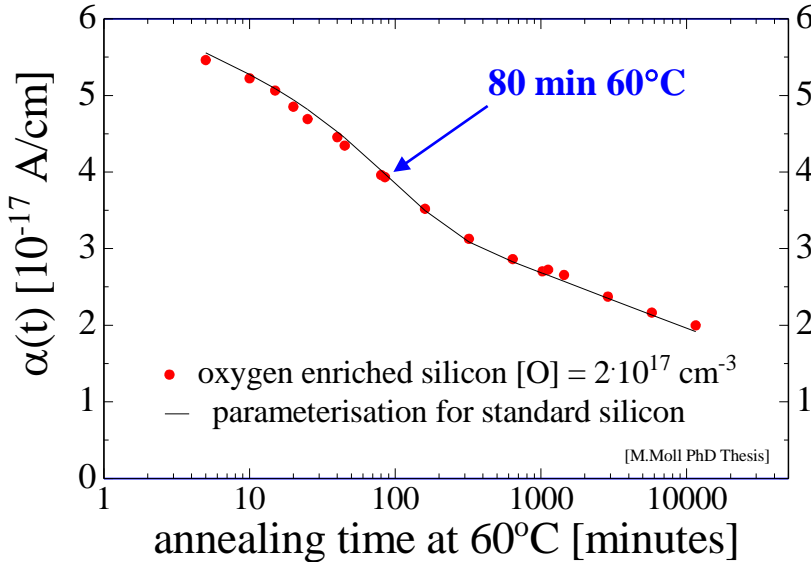
- Figure of Merit: Signal-to-Noise Ratio S/N. Radiation damage severely degrades the S/N, people get nervous below 10.



# Changes with time and temperature after irradiation (annealing)

## Leakage Current and $N_{\text{eff}}$ (after hadron irradiation)

.... with time (annealing):



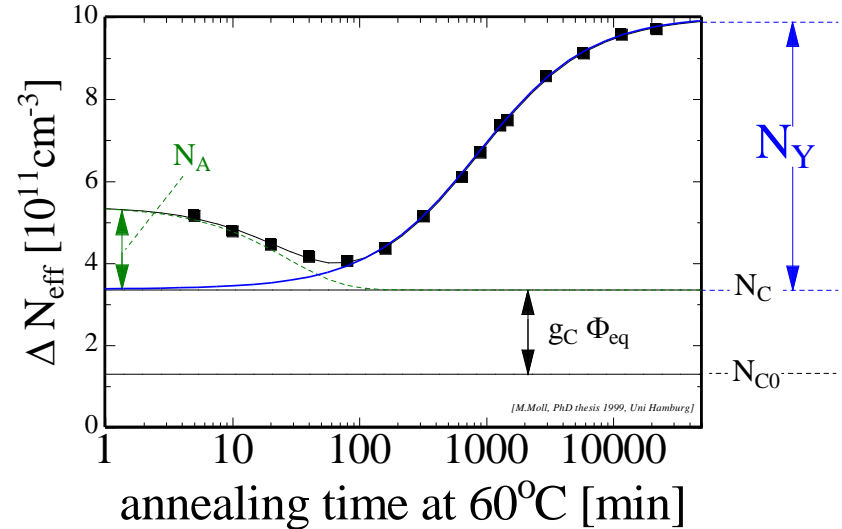
- Leakage current decreasing in time (depending on temperature)
- Strong temperature dependence

$$I \propto \exp\left(-\frac{E_g}{2k_B T}\right)$$

**Consequence:**

Cool detectors during operation!  
 Example:  $I(-10^\circ\text{C}) \sim 1/16 I(20^\circ\text{C})$

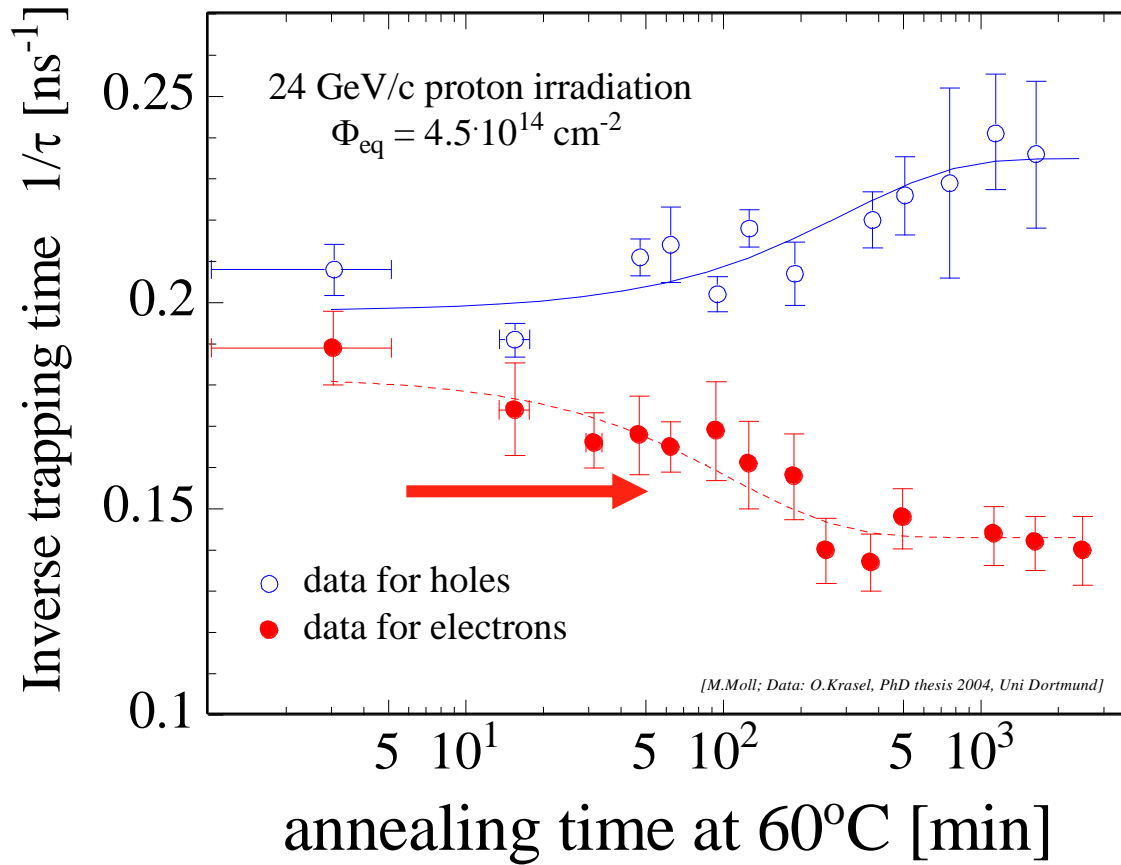
.... with time (annealing):



- Short term: “**Beneficial annealing**”
- Long term: “**Reverse annealing**”
- time constant depends on temperature:
  - ~ 500 years ( $-10^\circ\text{C}$ )
  - ~ 500 days ( $20^\circ\text{C}$ )
  - ~ 21 hours ( $60^\circ\text{C}$ )
- Consequence: **Detectors must be cooled even when the experiment is not running!**

# Change of inverse trapping time

Decrease of inverse trapping time  
( $1/\tau$ ) with annealing for electrons



# Approaches to develop radiation harder solid state tracking detectors

- Defect Engineering of Silicon

*Deliberate incorporation of impurities or defects into the silicon bulk to improve radiation tolerance of detectors*

- **Needs:** Profound understanding of radiation damage
  - microscopic defects, macroscopic parameters
  - dependence on particle type and energy
  - defect formation kinetics and annealing
- **Examples:**
  - Oxygen rich Silicon (DOFZ, Cz, MCZ, EPI)
  - Oxygen dimer & hydrogen enriched Si
  - Pre-irradiated Si
  - Influence of processing technology

- New Materials

- Silicon Carbide (SiC), Gallium Nitride (GaN)
- Diamond (CERN RD42 Collaboration)
- Amorphous silicon

- Device Engineering (New Detector Designs)

- p-type silicon detectors (n-in-p)
- thin detectors, epitaxial detectors
- 3D detectors and Semi 3D detectors, Stripixels
- Cost effective detectors
- Monolithic devices

## Scientific strategies:

- I. Material engineering
- II. Device engineering
- III. Change of detector operational conditions

CERN-RD39

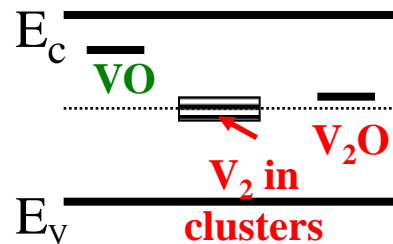
“Cryogenic Tracking Detectors”  
operation at 100-200K  
to reduce charge loss

# Oxygen Enrichment for Radiation Hardening

## RD48 (ROSE) and RD50 CERN Collaborations

**Main Hypothesis: Oxygen beneficial as sink of vacancies**

V-O<sub>i</sub> complex concentration increase  $\longrightarrow$  reduction of deeper levels  
mainly divacancy related



Typical oxygen concentration in Si:

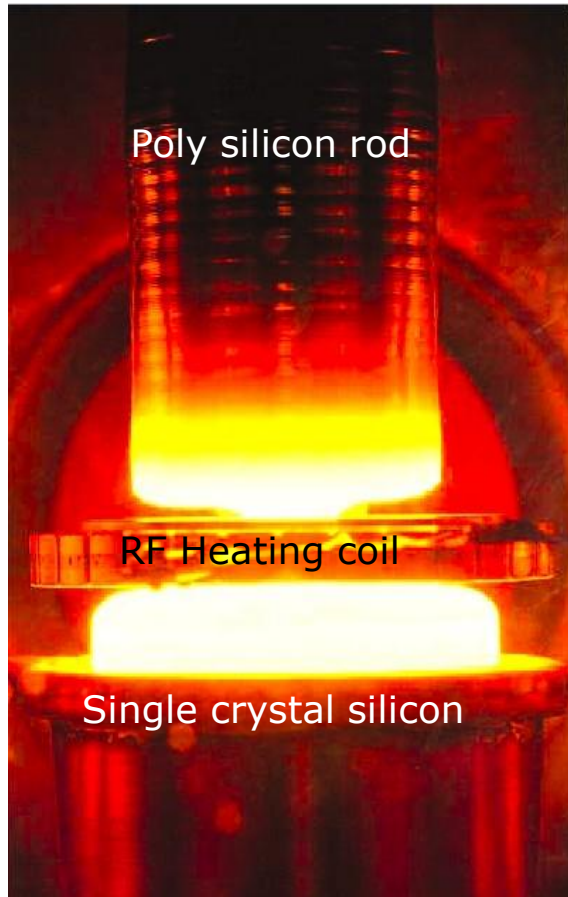
- FZ [O<sub>i</sub>] 10<sup>15</sup>cm<sup>-3</sup>
- Diffusion oxygenated FZ : DOFZ [O<sub>i</sub>] 10<sup>16</sup>-10<sup>17</sup>cm<sup>-3</sup>
- Czochralski Si: [O<sub>i</sub>] up to 10<sup>18</sup>cm<sup>-3</sup>

Note: as VO is a point defect the beneficial effect of oxygen is expected especially when cluster formation by irradiation is less important than point defect formation.

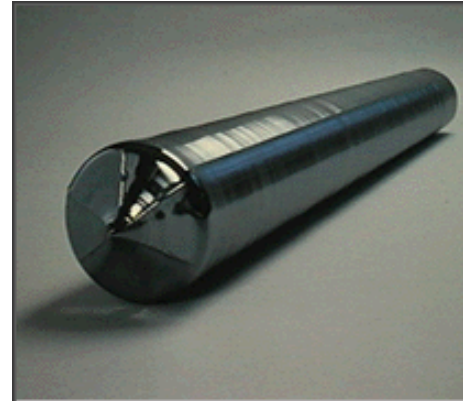
# Material: Float Zone Silicon (FZ)

## ■ Float Zone process

- Using a single Si crystal seed, melt the vertically oriented rod onto the seed using RF power and “pull” the **monocrystalline ingot**



## ■ Mono-crystalline Ingot



## ■ Wafer production

- Slicing, lapping, etching, polishing

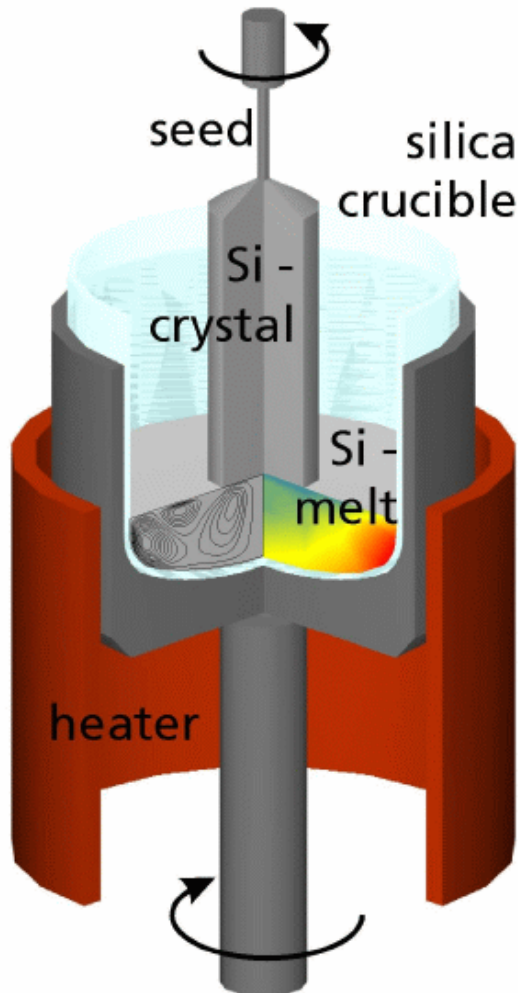


## ■ Highly pure crystal

- Low concentration of [O] and [C]  $10^{15}\text{cm}^{-3}$

### Czochralski silicon (Cz) & Epitaxial silicon (EPI)

#### ■ Czochralski silicon



- Pull Si-crystal from a Si-melt contained in a silica crucible while rotating.
- Silica crucible is dissolving oxygen into the melt ⇒ high concentration of O in CZ
- Material used by IC industry (cheap)
- Recent developments (~5 years) made CZ available in sufficiently high purity (resistivity) to allow for use as particle detector.

#### ■ Epitaxial silicon

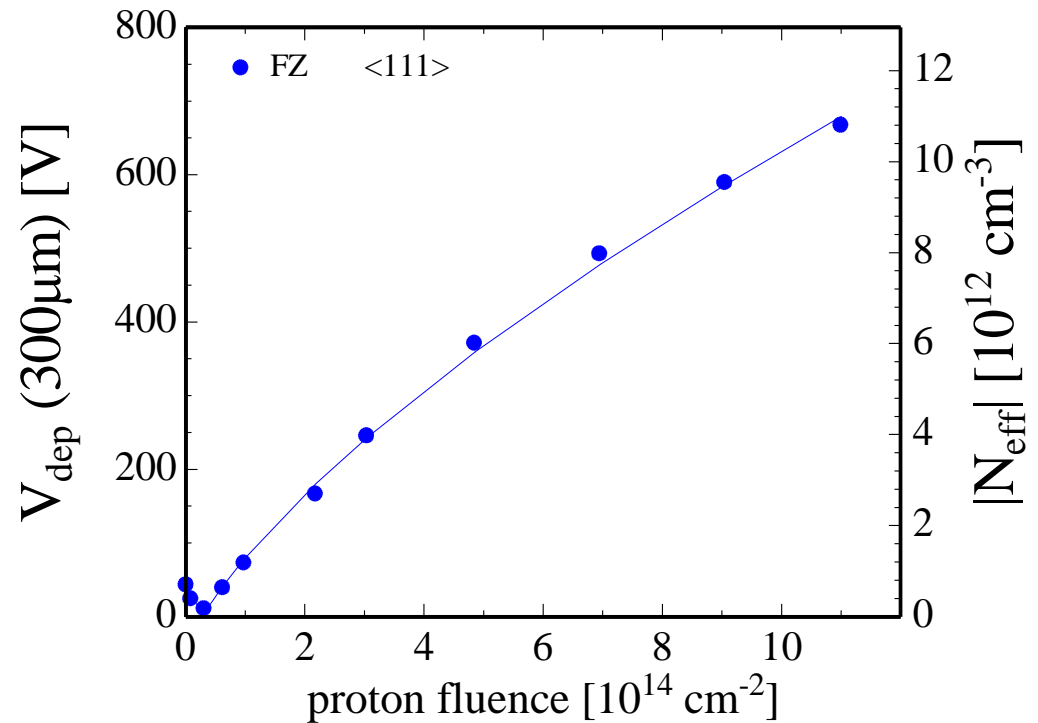
- Chemical-Vapor Deposition (CVD) of Silicon
- CZ silicon substrate used ⇒ in-diffusion of oxygen
- growth rate about 1 $\mu$ m/min
- excellent homogeneity of resistivity
- up to 150  $\mu$ m thick layers produced (thicker is possible)
- price depending on thickness of epi-layer but not extending ~ 3 x price of FZ wafer

# Standard FZ, DOFZ, MCz and Cz silicon

## 24 GeV/c proton irradiation

### • Standard FZ silicon

- type inversion at  $\sim 2 \times 10^{13}$  p/cm<sup>2</sup>
- strong  $N_{\text{eff}}$  increase at high fluence





# Standard FZ, DOFZ, MCz and Cz silicon

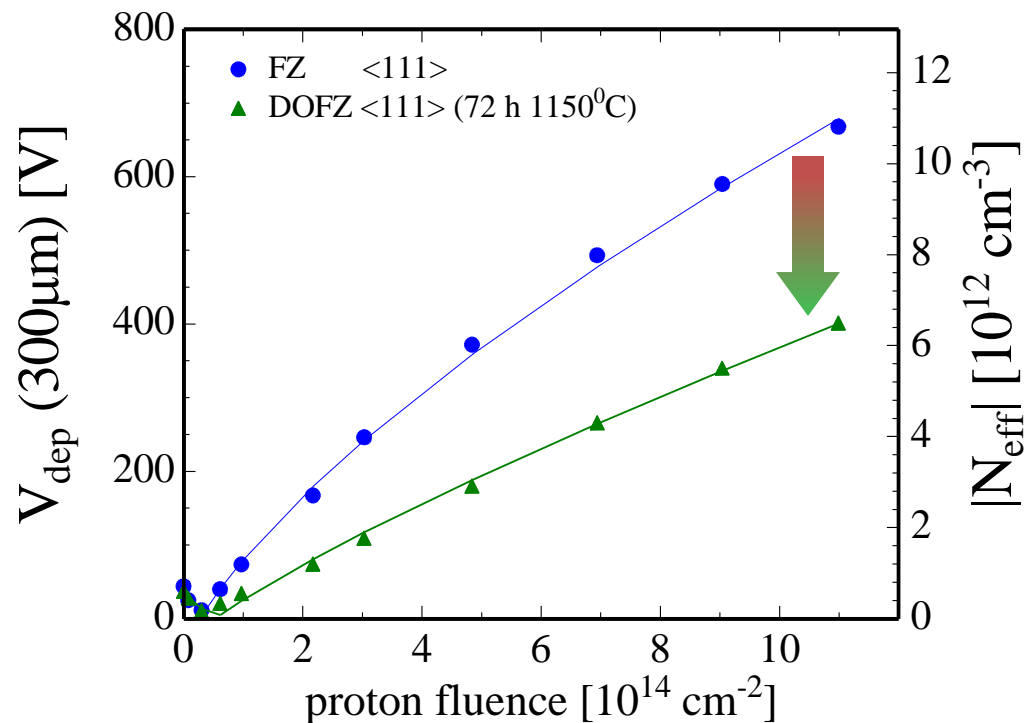
## 24 GeV/c proton irradiation

### • Standard FZ silicon

- type inversion at  $\sim 2 \times 10^{13}$  p/cm<sup>2</sup>
- strong  $N_{\text{eff}}$  increase at high fluence

### • Oxygenated FZ (DOFZ)

- type inversion at  $\sim 2 \times 10^{13}$  p/cm<sup>2</sup>
- reduced  $N_{\text{eff}}$  increase at high fluence



# Standard FZ, DOFZ, MCZ and Cz silicon

## 24 GeV/c proton irradiation

### • Standard FZ silicon

- type inversion at  $\sim 2 \times 10^{13}$  p/cm<sup>2</sup>
- strong  $N_{\text{eff}}$  increase at high fluence

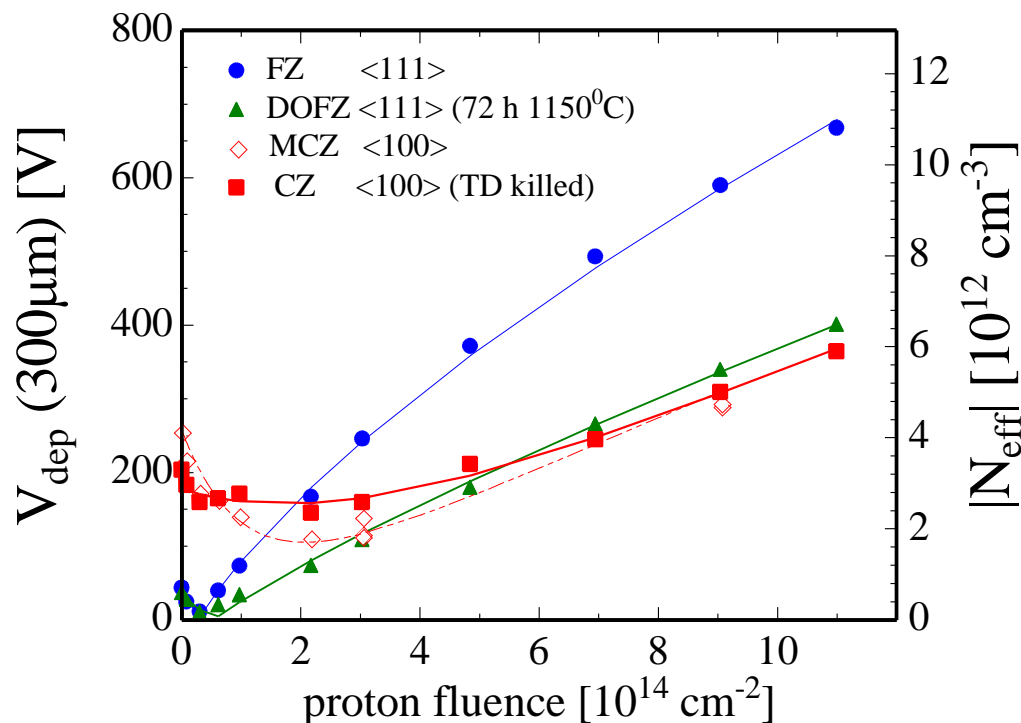
### • Oxygenated FZ (DOFZ)

- type inversion at  $\sim 2 \times 10^{13}$  p/cm<sup>2</sup>
- reduced  $N_{\text{eff}}$  increase at high fluence

### • CZ silicon and MCZ silicon

- “no type inversion” in the overall fluence range

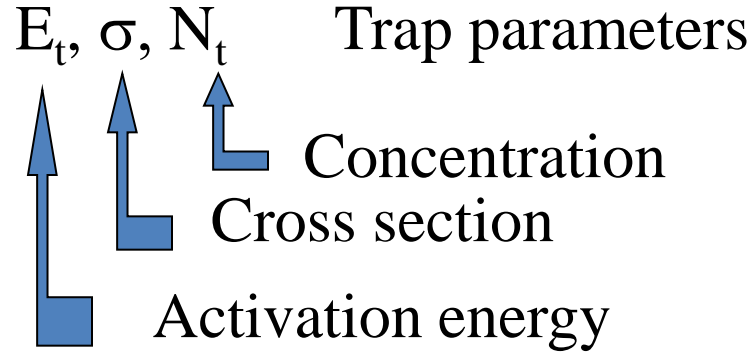
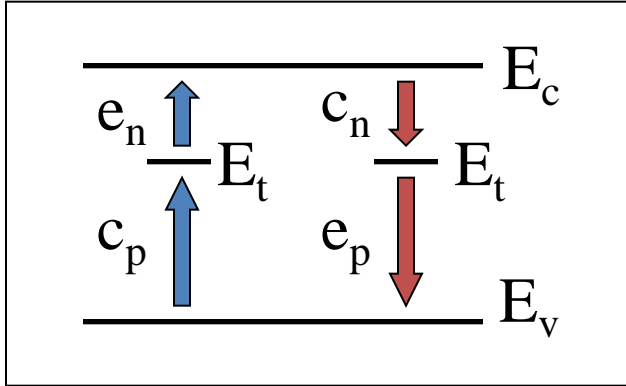
*(for experts: there is no “real” type inversion, a more clear understanding of the observed effects is obtained by investigating directly the internal electric field; look for: TCT, MCZ, double junction)*



### • Common to all materials (after hadron irradiation, not after $\gamma$ irradiation):

- reverse current increase
- increase of trapping (electrons and holes) within  $\sim 20\%$

# The Microscopic View: Defects in irradiated silicon

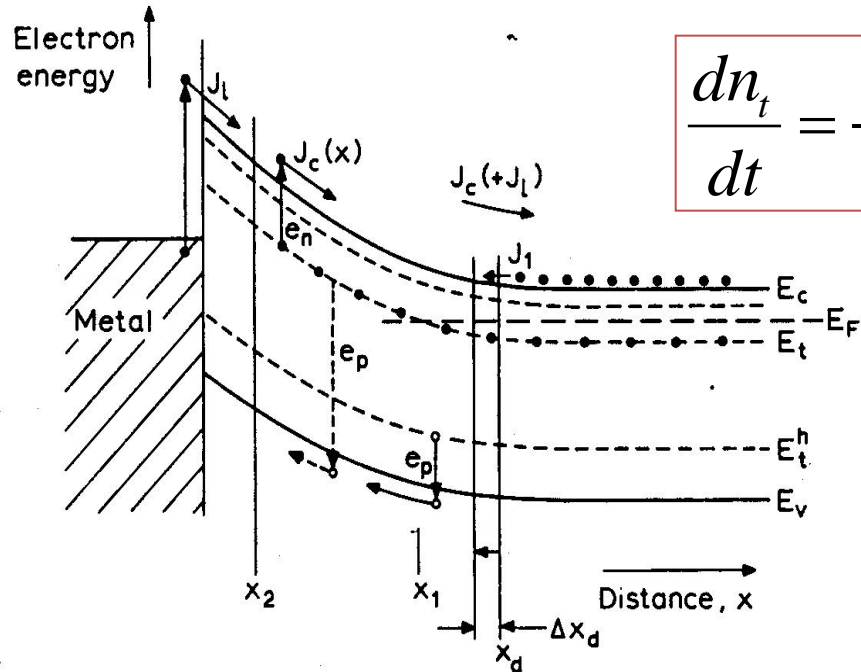


Emission coefficient:

$$e_n = N_c \sigma_n v_{th} \cdot e^{-\frac{E_c - E_t}{KT}}$$

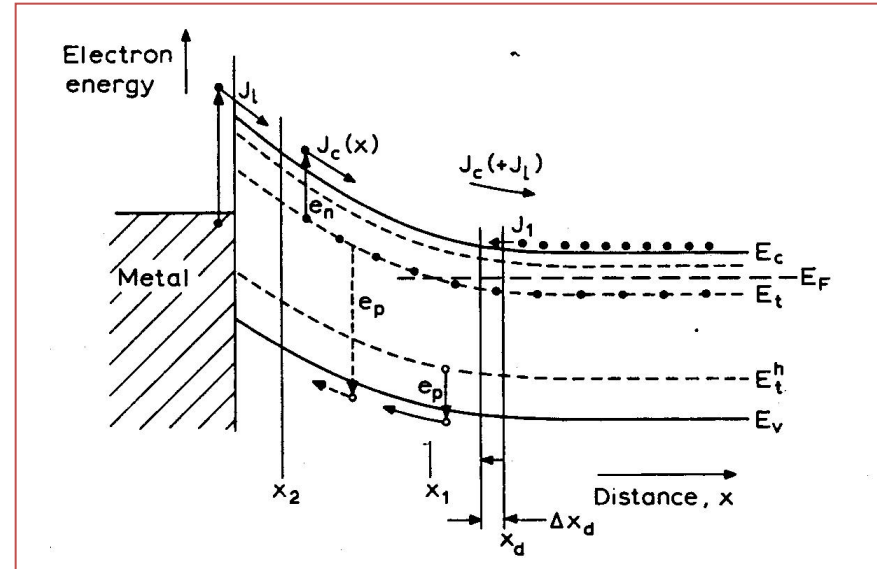
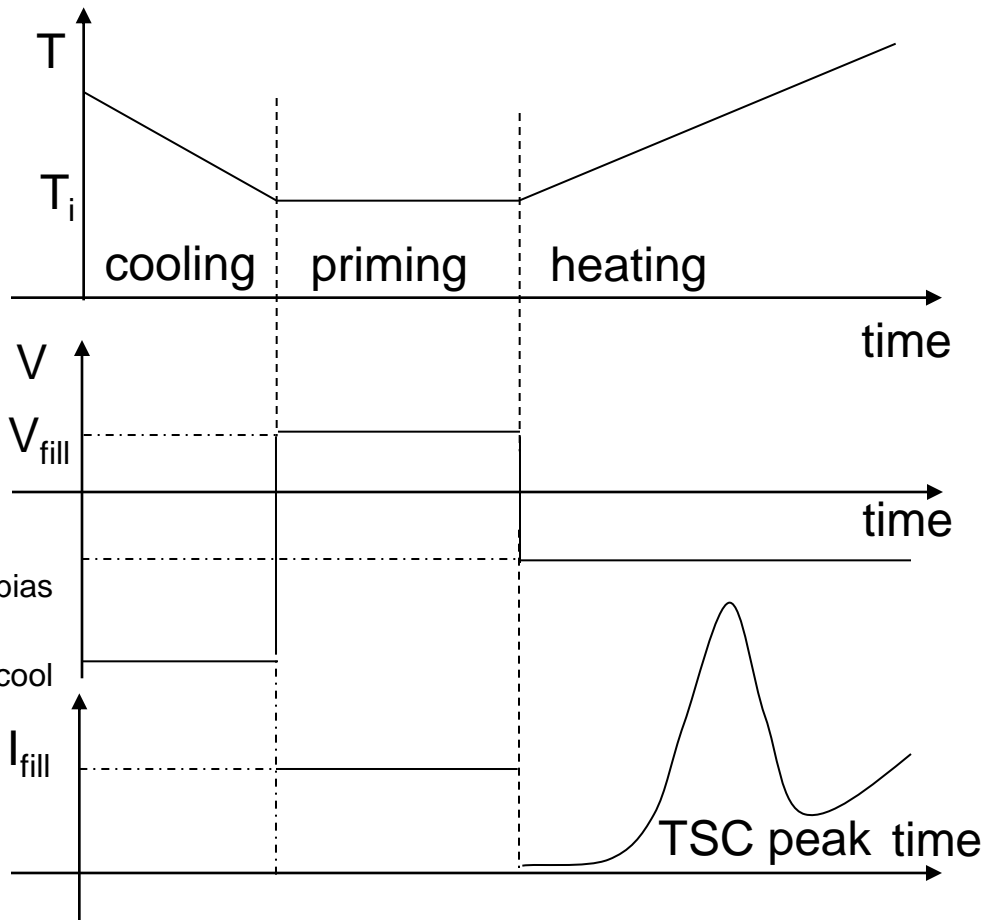
Capture coefficient :

$$c_n = n \sigma_n v_{th}$$



$$\frac{dn_t}{dt} = -e_n \cdot n_t$$

# Thermally Stimulated Current: TSC



-Cooling with applied reverse  $V_{cool}$  or null bias

-Forward voltage applied  $V_{fill}$  at  $T_i$  or illumination with optical source

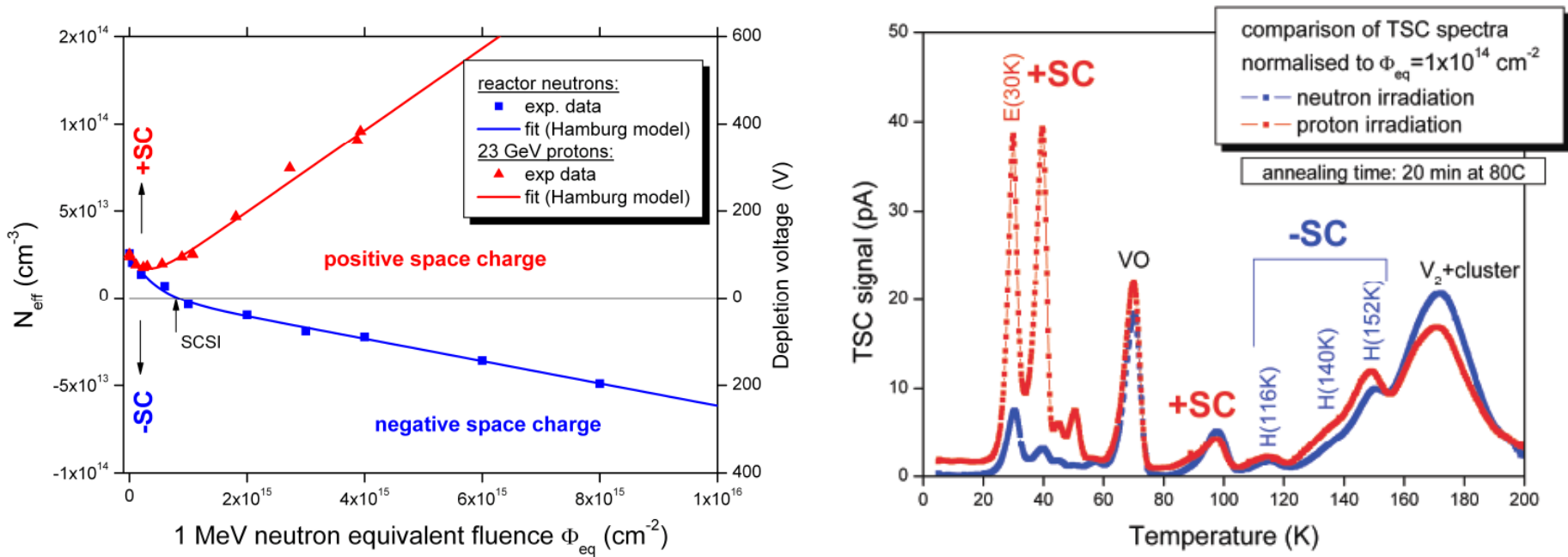
-  $V_{bias}$  applied

-Thermally stimulated current read-out

$$I_{TSC}(T) = -\frac{1}{2} q \cdot A \cdot N_t \cdot W \cdot e_n(T) \exp\left(-\frac{1}{b} \int_{T_i}^T e_n(T) dT\right)$$

# From microscopic to macroscopic: $N_{\text{eff}}$ changes explained with TSC

Epi-Si irradiated with 23 GeV protons and reactor neutrons



[Pintilie, Lindstroem, Junkes, Fretwurst, NIM A 611 (2009) 52–68]

- SCSI "Type Inversion" after neutrons but not after protons
- donor generation enhanced after proton irradiation

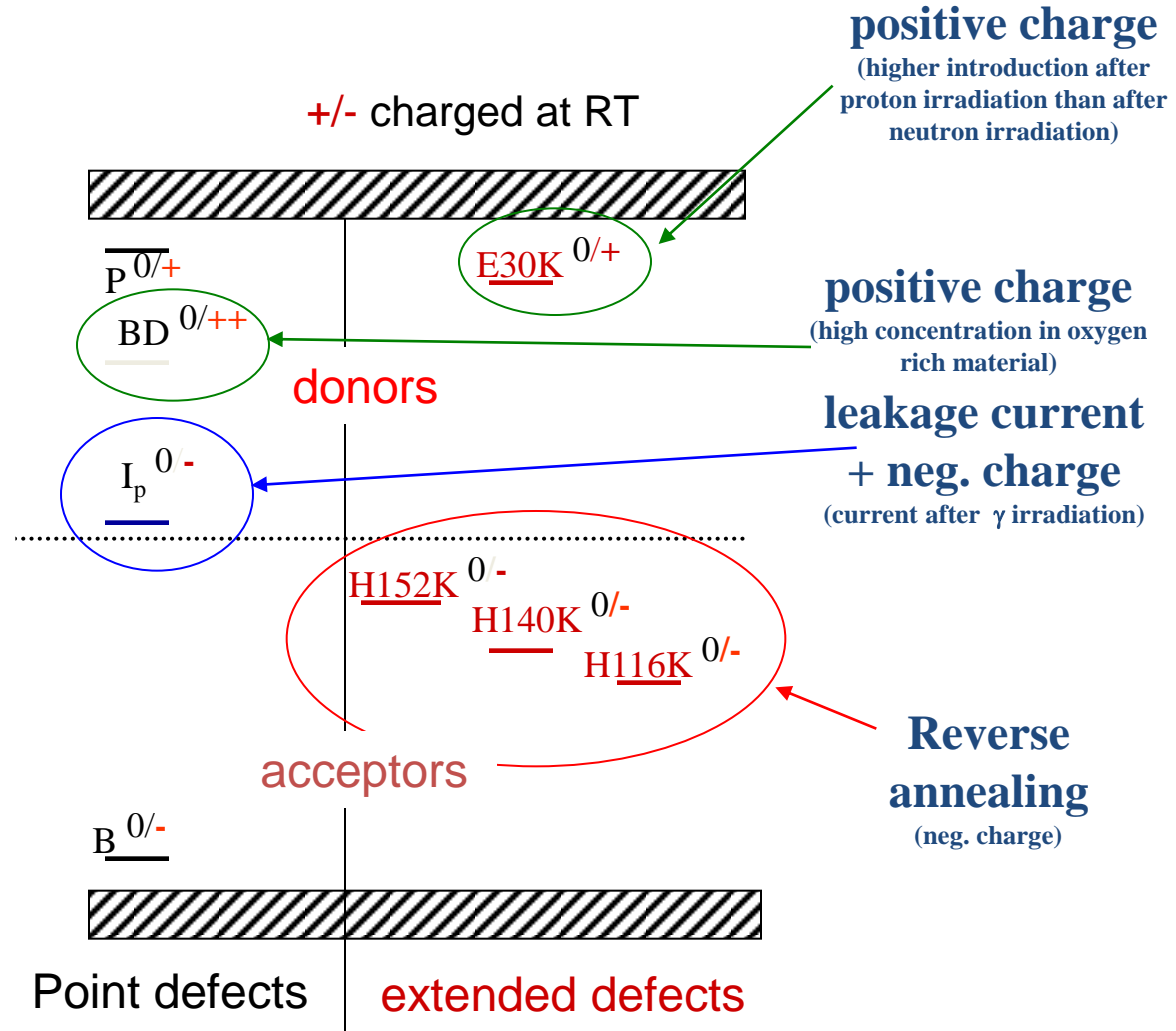
# Main Defects Affecting the Device Properties

## Point defects

- $E_i^{BD} = E_c - 0.225 \text{ eV}$
- $\sigma_n^{BD} = 2.3 \cdot 10^{-14} \text{ cm}^2$
- $E_i^I = E_c - 0.545 \text{ eV}$ 
  - $\sigma_n^I = 1.7 \cdot 10^{-15} \text{ cm}^2$
  - $\sigma_p^I = 9 \cdot 10^{-14} \text{ cm}^2$

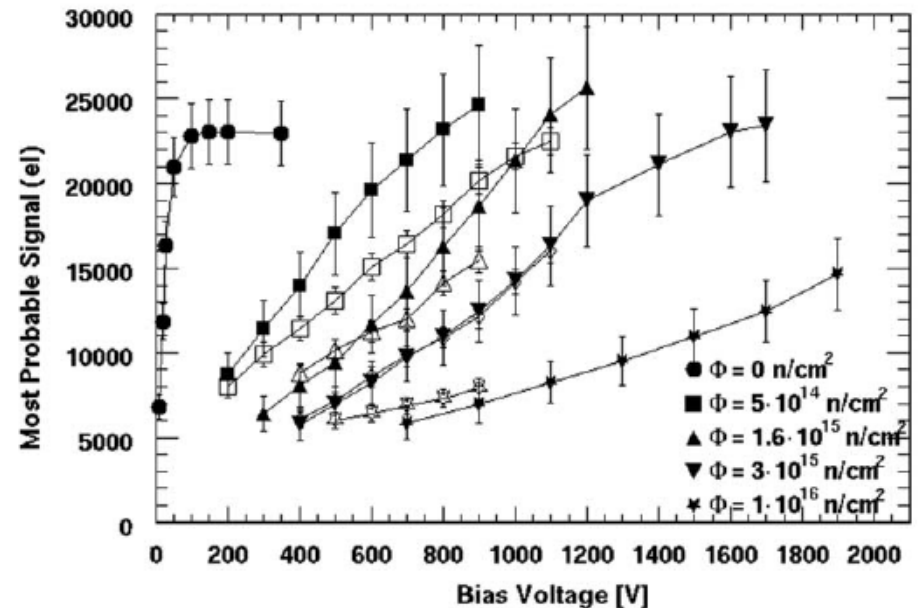
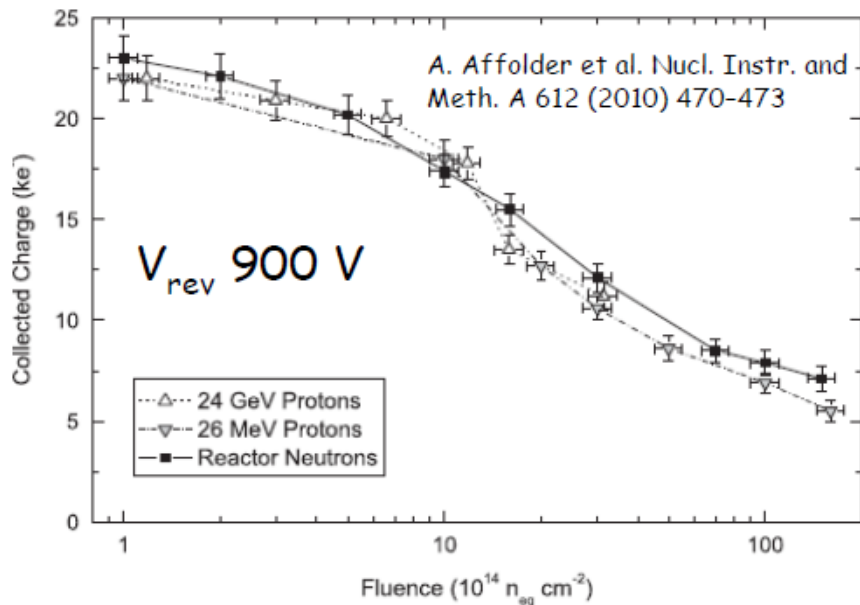
## Cluster related centers

- $E_i^{116K} = E_v + 0.33 \text{ eV}$
- $\sigma_p^{116K} = 4 \cdot 10^{-14} \text{ cm}^2$
- $E_i^{140K} = E_v + 0.36 \text{ eV}$
- $\sigma_p^{140K} = 2.5 \cdot 10^{-15} \text{ cm}^2$
- $E_i^{152K} = E_v + 0.42 \text{ eV}$
- $\sigma_p^{152K} = 2.3 \cdot 10^{-14} \text{ cm}^2$
- $E_i^{30K} = E_c - 0.1 \text{ eV}$
- $\sigma_n^{30K} = 2.3 \cdot 10^{-14} \text{ cm}^2$



# Charge collection in n on p FZ

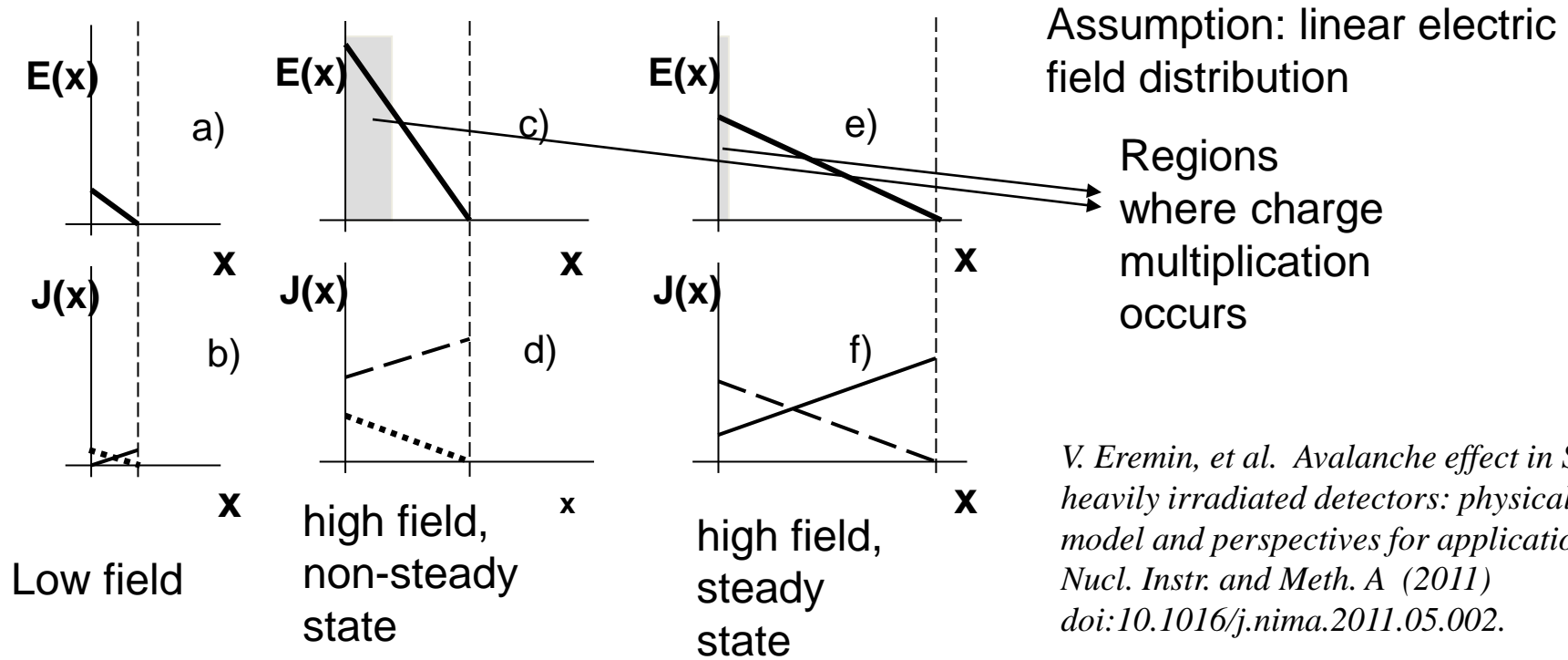
Advantage of n-side read-out: higher mobility of electrons with respect to holes. Better performances compared to standard p-side read-out already proved by n on n technology



I. Mandic et al. Nucl. Instr. And Meth. A 612 (2010) 474-477

- Charge still measurable after  $2 \times 10^{16} n_{eq} / \text{cm}^2$
- Collected charge higher than expected from  $V_{dep}$  and carriers trapping times at high fluences.
- at high voltages collected charge in irradiated detectors can be higher than unirradiated. Possible explanation: charge multiplication in high field region

# Modeling of charge multiplication effect on heavily irradiated n on p Si detectors



- at low field the current density is given by the bulk generated  $e^-$  and  $h^+$
- when a sufficiently enough high voltage is applied the electron multiplication occurs in a region close to the  $n^+$  contact which results in an avalanche injection of holes inside the bulk. The hole current density will be the sum of the bulk generated current and the avalanche hole injection.
- A fraction of this injected holes will be trapped inside the bulk contributing to a positive  $N_{eff}$  and thus a higher depletion depth



# Space Charge Limited Avalanche (SCLA)

Combination of three processes:

- avalanche hole generation,
- hole injection into the detector bulk,
- hole trapping to the deep levels of radiation induced defects in the bulk

gives rise to the negative feedback that:

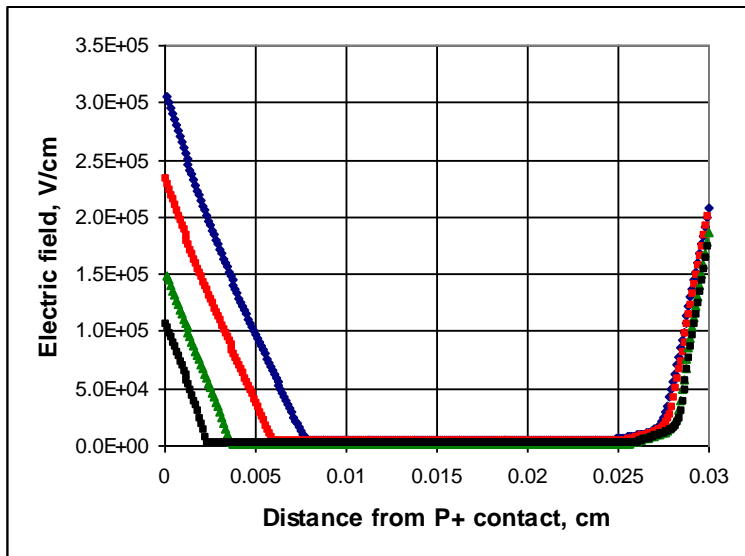
- reduces and stabilizes maximum electric field at n+ contact,
- this stabilization takes place in both designs – pad and strip,  
in strips for any strip width to pitch ratio;
- stabilizes the avalanche multiplication,
- prevents the detector breakdown,
- smoothes out the signal on voltage and current on voltage characteristics.

# Electric Field simulation with consideration of current focusing in strip detectors

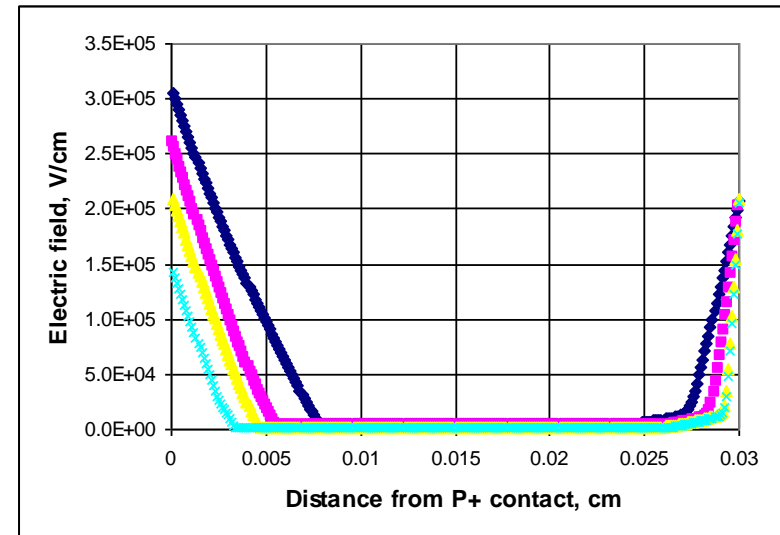
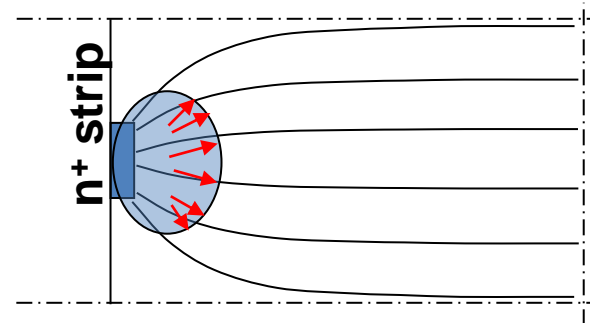
- The electric field was simulated with the PTI model\* which takes into account two effective energy levels: a midgap donor and a migap acceptor
- A correction for electric field focusing has been introduced

**NO electric field focusing**  
(PAD configuration)

$F_n = 1 \times 10^{16} \text{ cm}^{-2}$ ,  $V = 1500, 1000, 700, 500\text{V}$



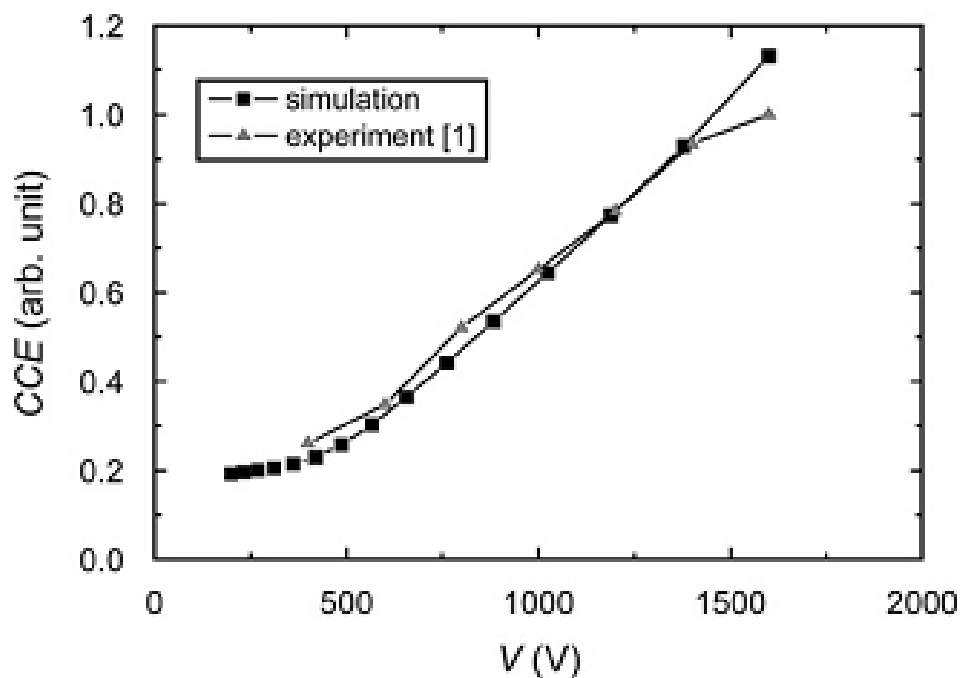
**electric field focusing**



\*V. Eremin, E. Verbitskaya, Z. Li, Nucl. Instr. and Meth. A 426 (2002) 537.

# Correlation between experimental data and calculated CCE

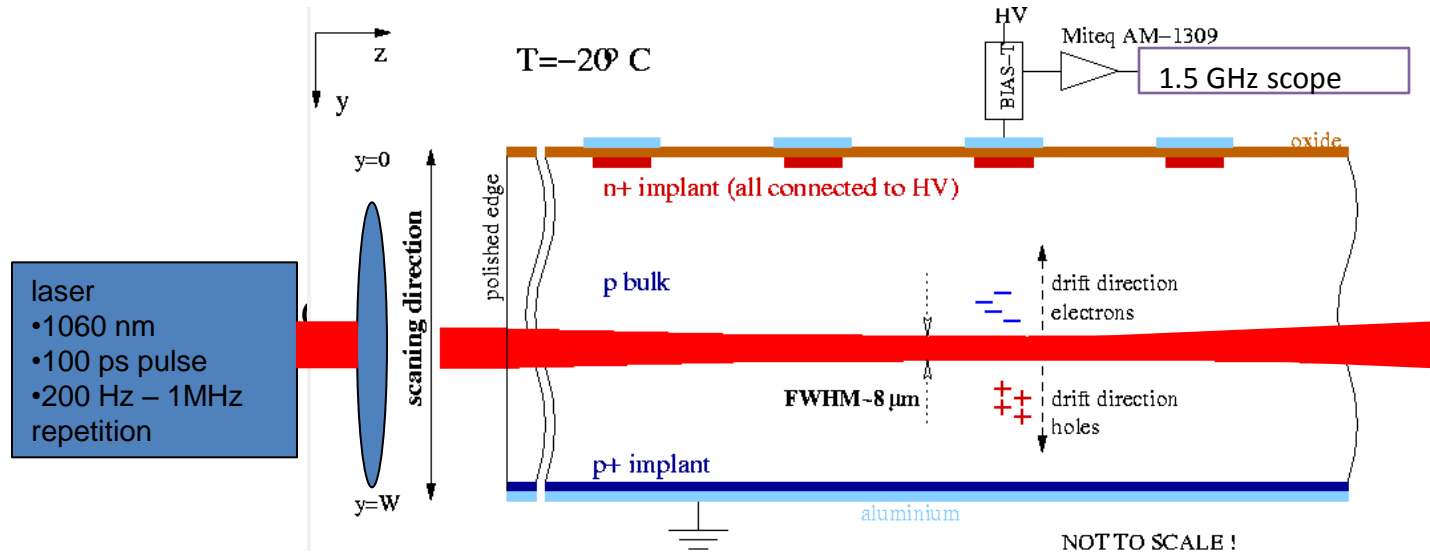
$$F_n = 3 \times 10^{15} \text{ cm}^{-2}$$



V. Eremin, et al.  
*Avalanche effect in Si  
heavily irradiated  
detectors: physical  
model and perspectives  
for application. Nucl.  
Instr. and Meth. A  
(2011)  
doi:10.1016/j.nima.201  
1.05.002.*

In plot: I. I. Mandić, et al. *NIM A* 612 (2010) 474

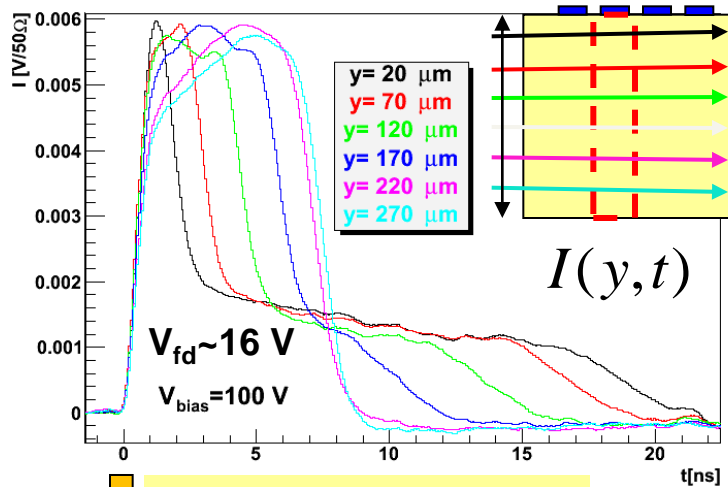
# Edge-Transient Current Technique (TCT): a tool to estimate the electric field distribution within the thickness of the detector



- The detector is illuminated by a collimated pulsed infrared laser beam
- The beam is focused below the readout strip and is scanned along the thickness
- At each depth the current transient is sampled by a wide bandwidth oscilloscope

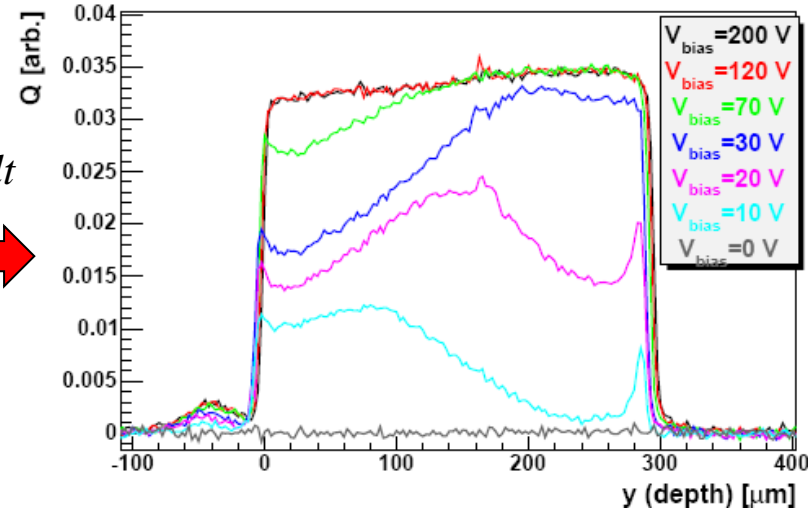
From the analysis of the current transients the carrier drift velocity and efficiency can be extracted

# Charge collection and velocity profiles



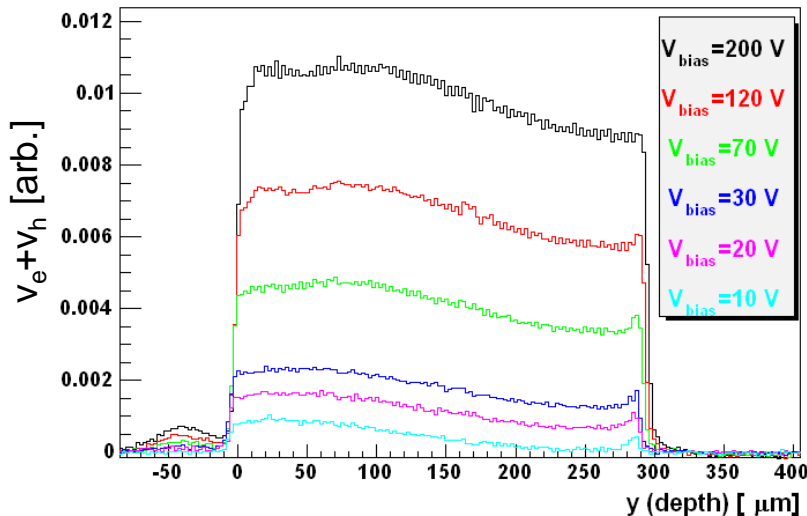
$$Q(y) = \int_0^{25\text{ns}} I(y, t) dt$$

## CHARGE COLLECTION PROFILE

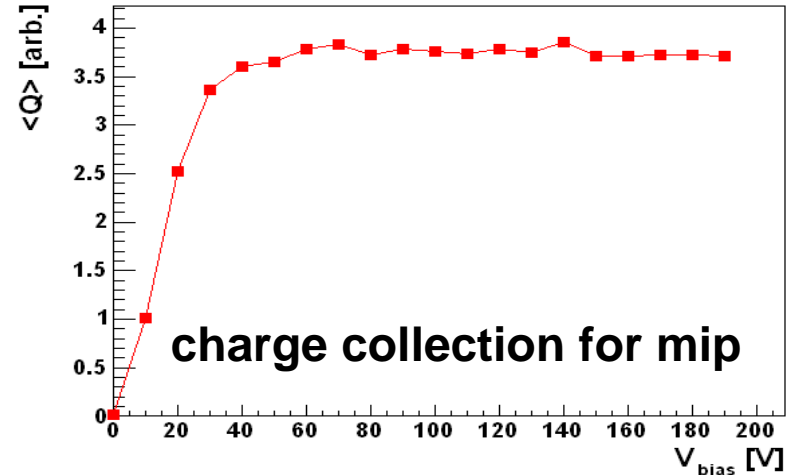


$$I(y, t \sim 0) \propto v_e + v_h$$

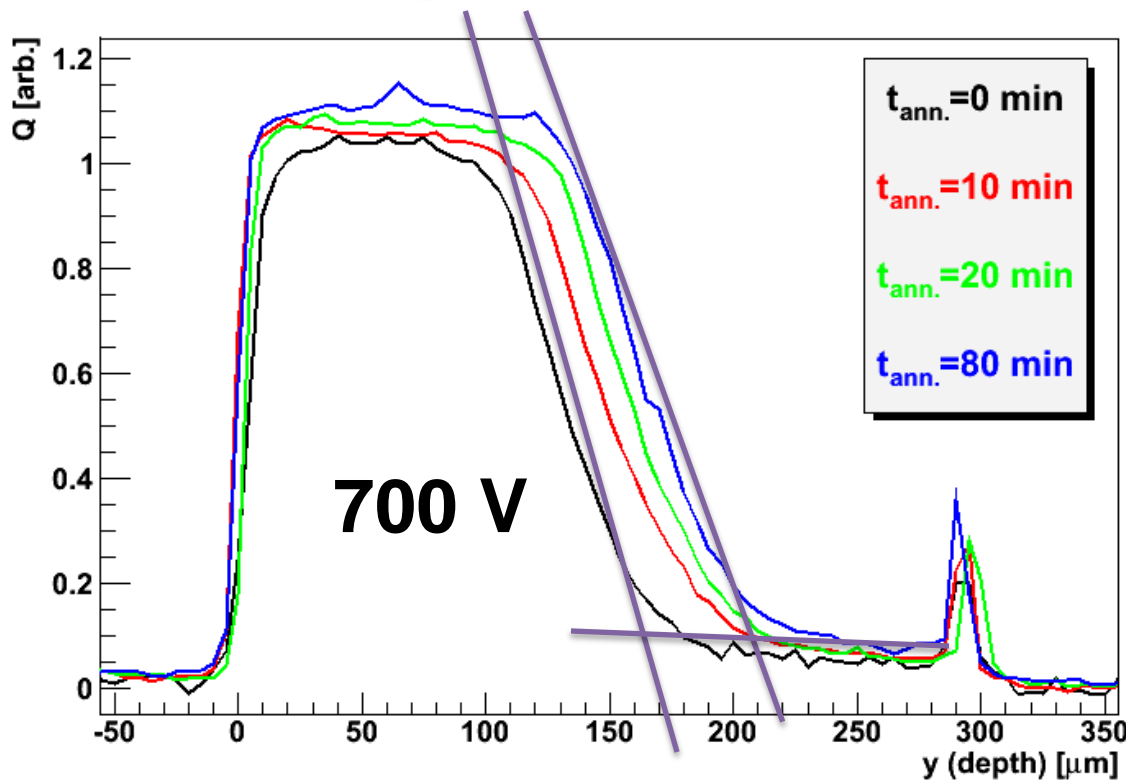
## VELOCITY PROFILE



$$Q_{mip} \propto \langle Q \rangle = \int_0^W Q(y) dy$$



# HPK ( $\Phi_{eq} = 10^{15} \text{ cm}^{-2}$ ) – beneficial annealing



$$N_{\text{eff}} \approx g_c \cdot \Phi_{eq} + N_{\text{eff}0} \quad , \quad g_c = 2 \cdot 10^{-2} \text{ cm}^{-2}$$

$$V_{fd} (80 \text{ min at } 60^\circ \text{C}) \approx 1600 \text{ V}$$

↓

$$\text{predicted: } y_{\text{act}}(700 \text{ V}) \approx 200 \text{ } \mu\text{m}$$

$$\text{measured: } y_{\text{act}}(700 \text{ V}) = 205 \text{ } \mu\text{m}$$

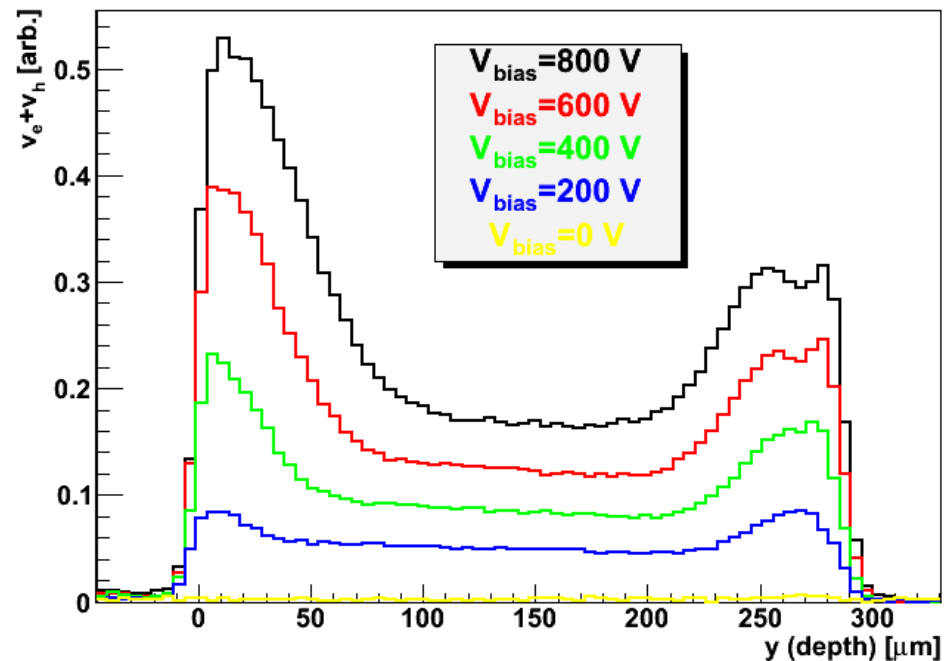
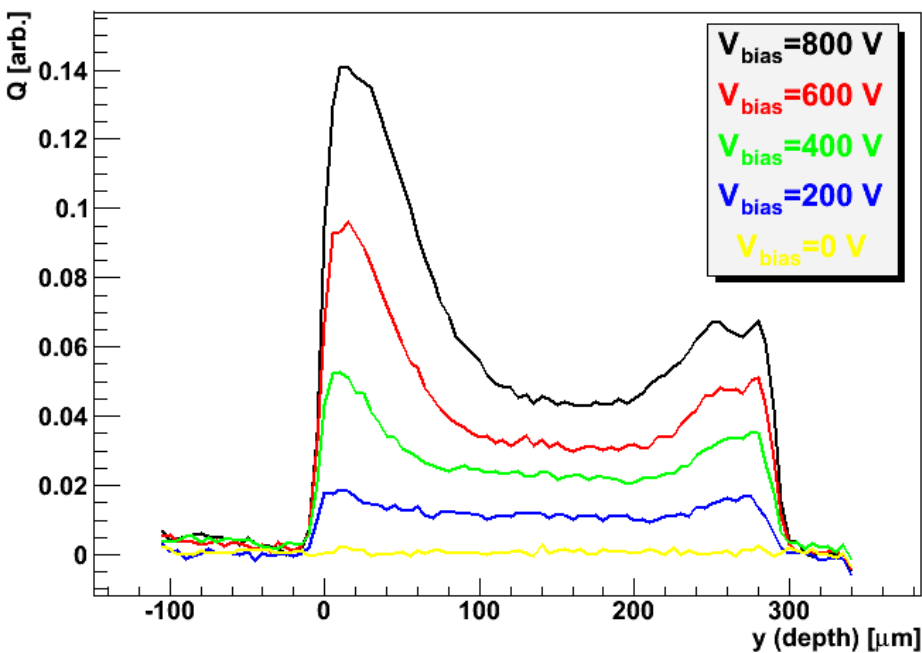
$$\Delta N_{\text{eff}} \approx N_{\text{eff}} \cdot \left[ \frac{y_{\text{act}}(0 \text{ min})}{y_{\text{act}}(80 \text{ min})} \right]^2$$

$$g_a \approx \frac{\Delta N_{\text{eff}}}{\Phi_{eq}} \approx 0.008 \text{ cm}^{-1}$$

- the predicted active region ( $N_{\text{eff}} = \text{const.}$ ) is very close to the measured
- A small peak at the back junction appears (double junction)

***In agreement with expectations based on RD48 and RD50 data – up to  $10^{15} \text{ cm}^{-2}$  the device behaves in accordance with expectations derived at lower fluences.***

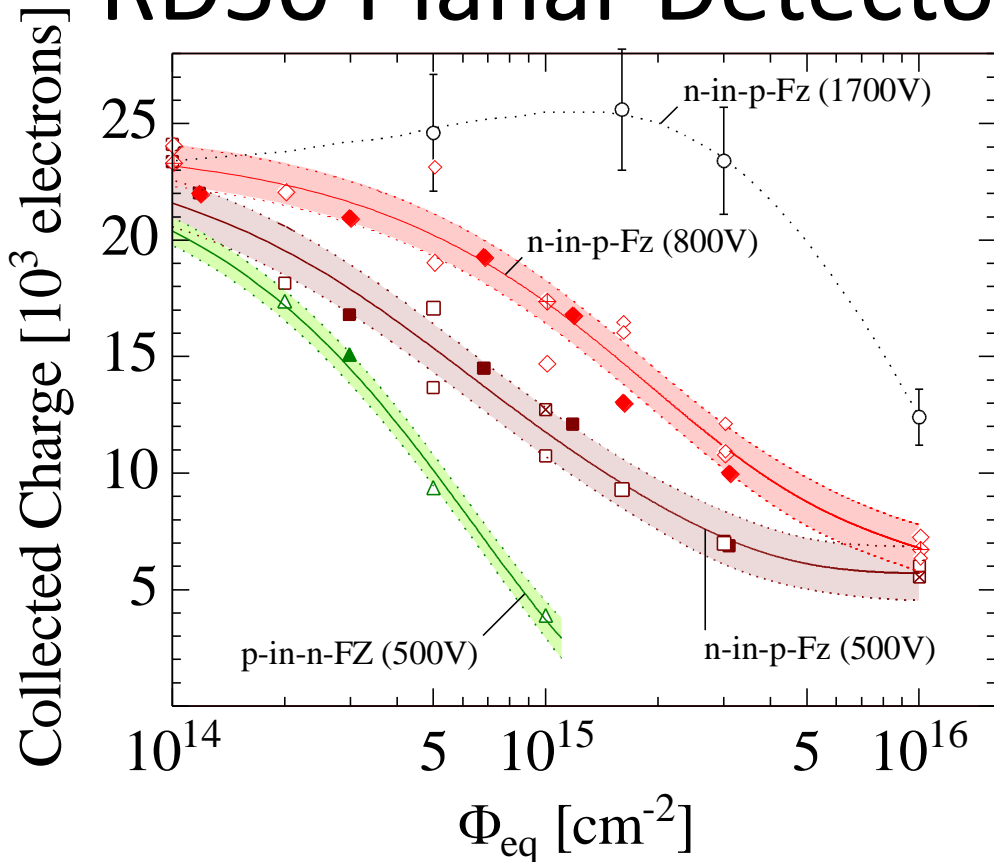
# HPK ( $\Phi_{eq} = 10^{16} \text{ cm}^{-2}$ )



Electric field is established in the whole detector – more pronounced double junction profile

An important contribution to the collected charge from “non active” regions which brings extra signal with respect of the predicted values from  $V_{\text{dep}}$ . This contribution adds up to the one due to charge multiplication

# RD50 Planar Detector Compilation



## FZ Silicon Strip Sensors

- n-in-p (FZ), 300 $\mu\text{m}$ , 500V, 23GeV p
- n-in-p (FZ), 300 $\mu\text{m}$ , 500V, neutrons
- ⊠ n-in-p (FZ), 300 $\mu\text{m}$ , 500V, 26MeV p
- ◆ n-in-p (FZ), 300 $\mu\text{m}$ , 800V, 23GeV p
- ◇ n-in-p (FZ), 300 $\mu\text{m}$ , 800V, neutrons
- ⊠ n-in-p (FZ), 300 $\mu\text{m}$ , 800V, 26MeV p
- n-in-p (FZ), 300 $\mu\text{m}$ , 1700V, neutrons
- ▲ p-in-n (FZ), 300 $\mu\text{m}$ , 500V, 23GeV p
- △ p-in-n (FZ), 300 $\mu\text{m}$ , 500V, neutrons

RD50 - M. Moll

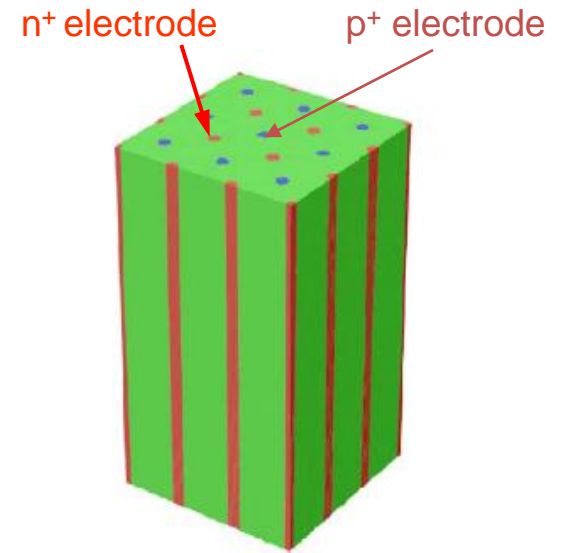
- p-in-n fades away well before  $10^{15} N_{eq}$
- n-in-p still gets 50% charge at  $10^{16} N_{eq}$  at high bias voltages
- n-in-p benefits from charge multiplication (at high bias voltages)
- CM effect also seen for p-in-n (but less strong in partial depletion mode)
- n-in-p (n-in-n) superior material for high radiation environments



# 3D detectors

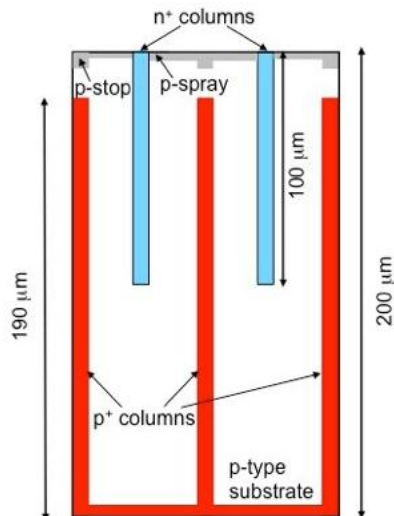
- The charge is collected in the narrow region in between the columns (50 – 100  $\mu\text{m}$ )  $\rightarrow$  radiation hard
- the depletion occurs laterally in between the columns  $\rightarrow$  low  $V_{\text{dep}}$

Conceptual design\*

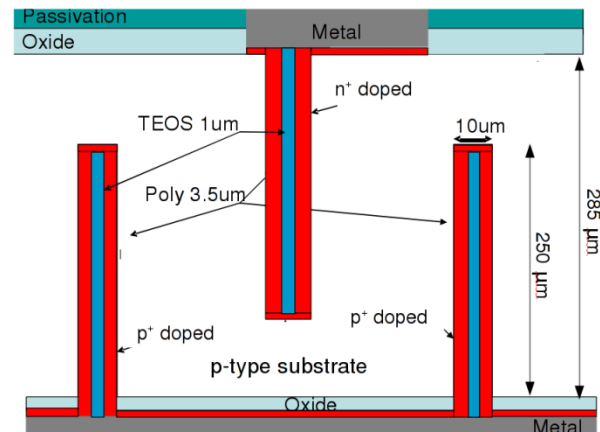


**Simplified version of the original design:  
double sided 3D**

FKB – Trento design



CNM – Barcelona design



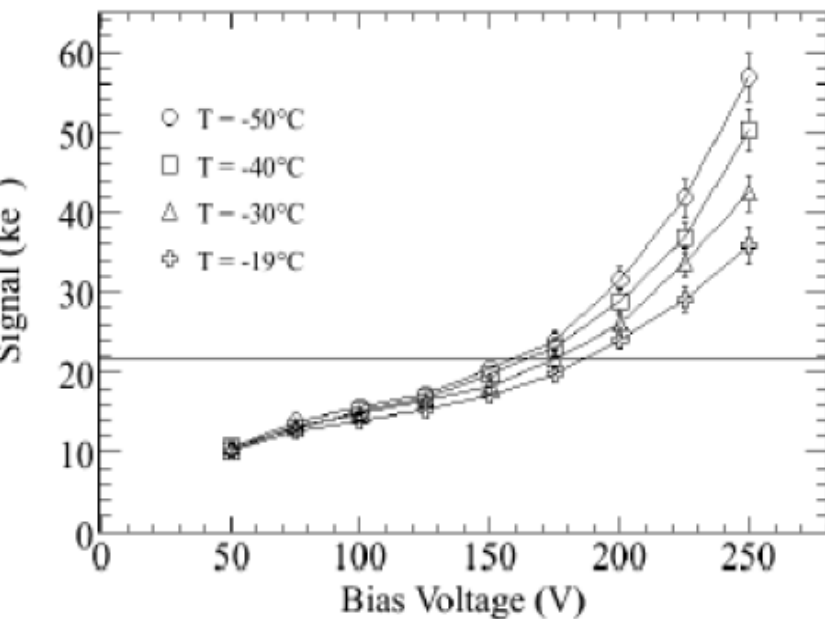
\*S.I. Parker et al., NIMA 395 (1997) 328

# Charge collection measurements

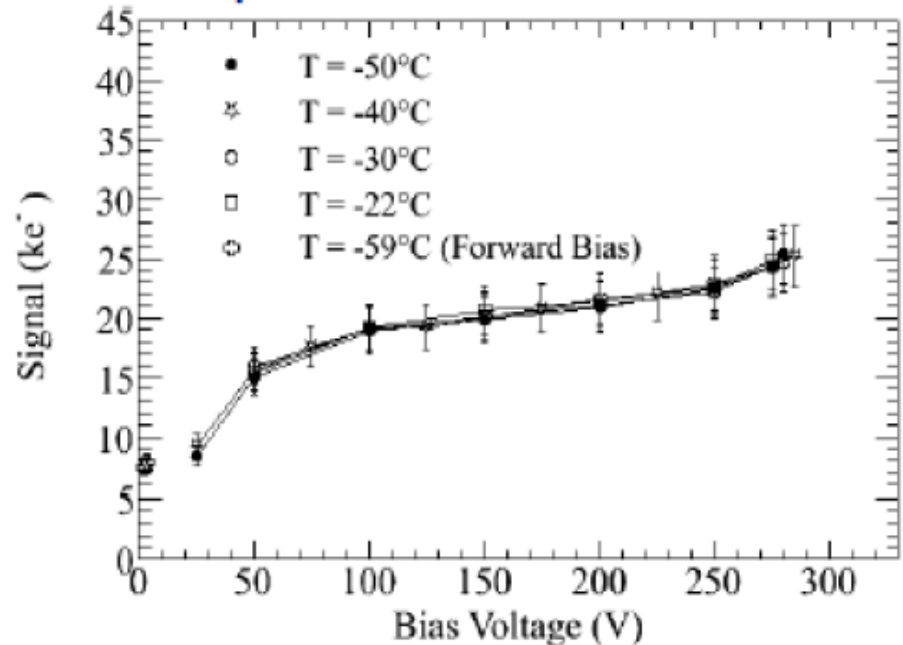
- CNM samples irradiated at the proton cyclotron Karlsruhe with 25 MeV protons
- Charge measurements performed with  $^{90}\text{Sr}$  beta source and LCHb "beetle" readout chip (ALIBAVA) at varying temperatures

Samples irradiated at  $2 \times 10^{15} \text{ n}_{\text{eq}}/\text{cm}^2$

n-in-p



p-in-n

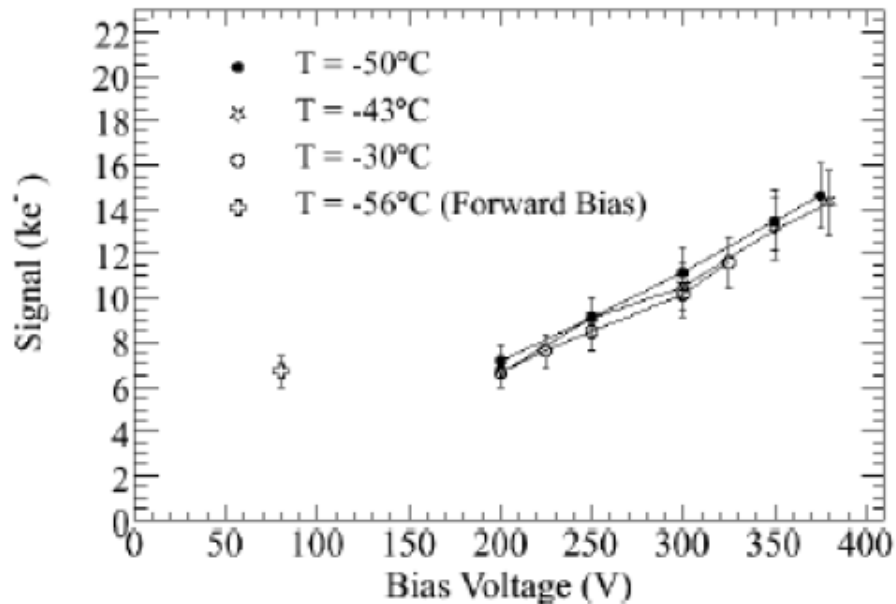


- Charge multiplication above 150 V
- Lower temperatures: higher charge multiplication

- Charge multiplication above 260 V?
- No temperature dependence

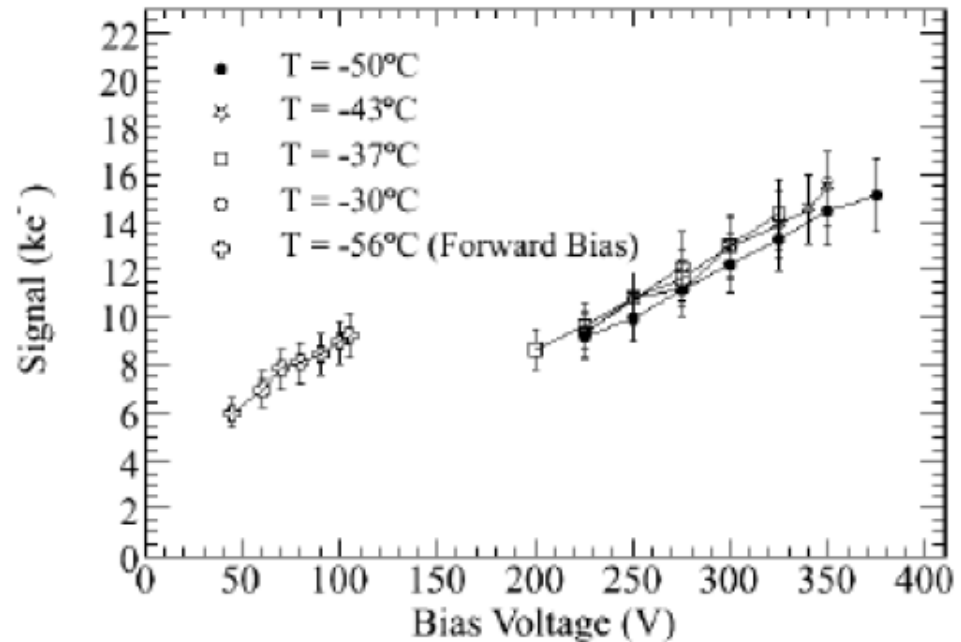
# Samples irradiated at $2 \times 10^{16} \text{ n}_{\text{eq}}/\text{cm}^2$

n-in-p



15 ke<sup>-</sup> at 380 V reverse bias

p-in-n



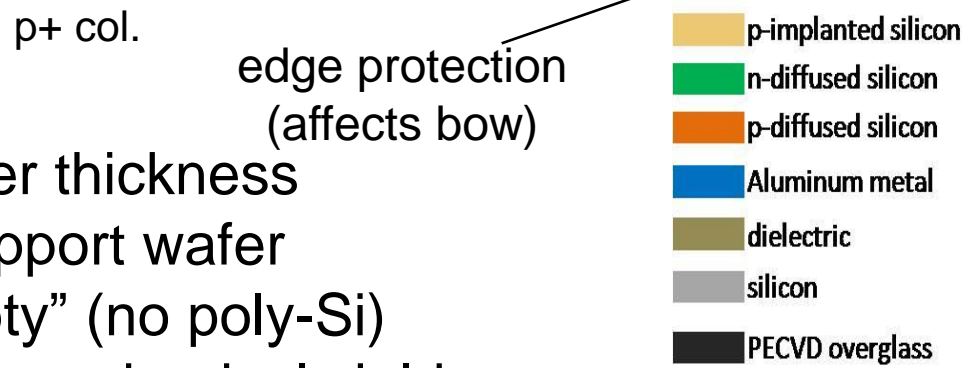
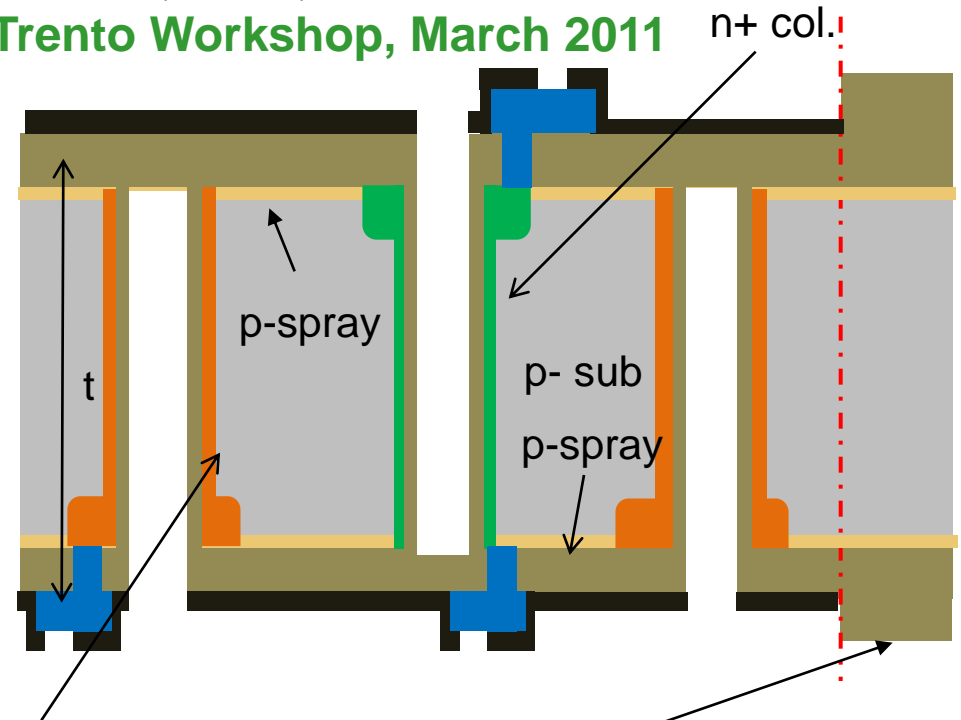
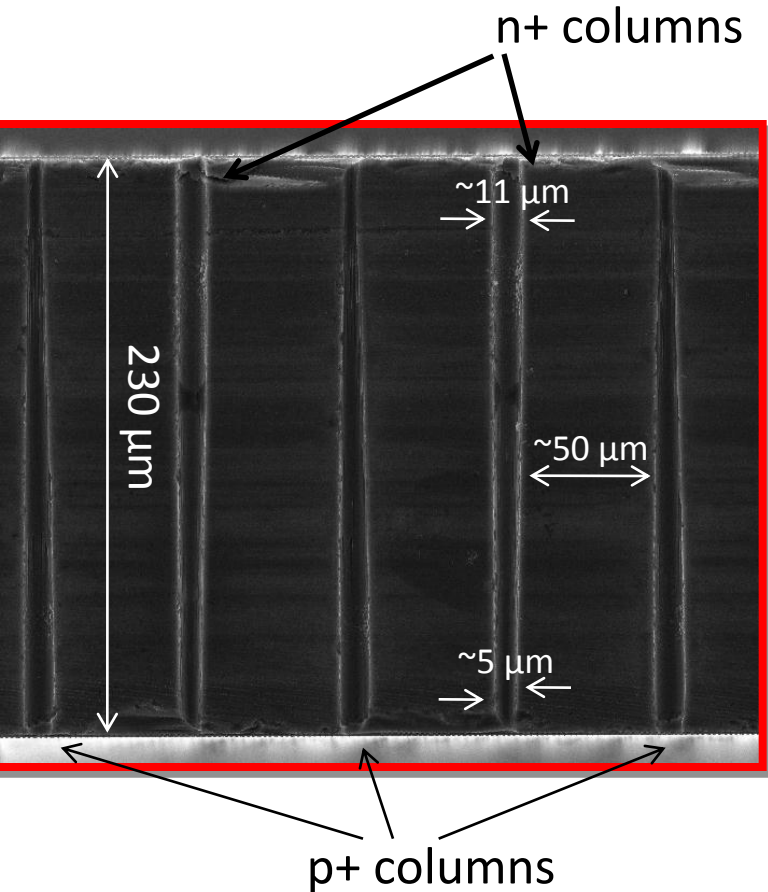
15 ke<sup>-</sup> at 350 V reverse bias

- The maximum signal for n-type and p-type substrate is the same
- No significant temperature dependence

# 3D-DTC with passing through columns at FBK

E. Vianello, et al.,

6<sup>th</sup> Trento Workshop, March 2011



- column depth equal to the wafer thickness
- full double side process, no support wafer
- holes ( $\sim 11 \mu\text{m}$  diam.) are “empty” (no poly-Si)
- edge protection to improve the mechanical yield

# Conclusions

- The RD50 collaboration is working on the development of radiation hard detectors for high luminosity collider (e.g. HC-LHC)
- Charge collection efficiency measurements on n-on p FZ silicon detectors show very good performances, better than expected by simulations
- At high voltages the collected charge can be higher than in unirradiated devices → charge multiplication
- A model was proposed to explain the self-stabilizing effect for charge multiplication in highly irradiated detectors
- Edge-TCT measurements were performed in order to estimate the electric field distribution along the thickness of the sample. A significant amount of charge is collected outside of the active volume
- Double sided 3D detectors were produced in the framework of the collaboration (CNM, FBK)
- Charge collection measurements on irradiated 3D detector show:
  - Charge multiplication effects (at lower voltages for p-type substrate)
  - High charge (15 ke-) measured after HL-LHC fluence
- Full 3D detectors (passing columns) are under development within the collaboration